Thermodynamical properties of planetary fluid envelopes

Valerio Lucarini [v.lucarini@reading.ac.uk]

Department of Meteorology & Department of Mathematics, University of Reading,

Reading, UK

Klaus Fraedrich & Francesco Ragone

Meteorologisches Institut, Klimacampus, University of Hamburg, Grindelberg 5,

Hamburg Germany

Abstract

In this paper we exploit two equivalent formulations of the average rate of material entropy production in a planetary system to propose an approximate splitting between contributions due to vertical and eminently horizontal processes. Our approach is based only upon 2D radiative fields at the surface and at the top of atmosphere of a general planetary body. Using 2D fields at the top of atmosphere alone, we derive lower bounds to the rate of material entropy production and to the intensity of the Lorenz energy cycle. By introducing a measure of the efficiency of the planetary system with respect to horizontal thermodynamical processes, we provide insight on a previous intuition on the possibility of defining a baroclinic heat engine extracting work from the meridional heat flux. The approximate formula of the material entropy production is verified and used for studying the global thermodynamic properties of climate models (CMs) included in the PCMDI/CMIP3 dataset in pre-industrial climate conditions. It is found that about 90% of the material entropy production is due to vertical processes such as convection, whereas the large scale meridional heat transport contributes only about 10%. This suggest that the traditional 2-box models used for providing a minimal representation of entropy production in planetary systems are not appropriate, while a basic – but conceptually correct – description can be framed in terms of a 4-box model. The total material entropy production is typically 55 $mWK^{-1}m^{-2}$, with discrepancies of the order of 5% and CMs' baroclinic efficiencies are clustered around 0.055. The lower bounds on the intensity of the Lorenz energy cycle featured by CMs are found to be around 1.0-1.5Wm^{-2}, which implies that the derived inequality is rather stringent as the lower bound is about 50% of the actual value. When looking at the variability and co-variability of the considered thermodynamical quantities, the agreement among CMs is worse, suggesting that the description of feedbacks is more uncertain. The contributions to material entropy production from vertical and horizontal processes are positively correlated, so that no compensation mechanism seems in place. Quite consistently among CMs, the variability of the efficiency of the system is a better proxy for variability of the entropy production due to horizontal processes than that of the large scale heat flux. Observational estimates of the climatology of the thermodynamical bounds are derived for Earth, Mars, Titan and Venus from very coarse data on the radiative fluxes at the top of the atmosphere. We discover that, once a suitable rescaling based upon the energy input is performed, these celestial objects share bounds that agree within one order of magnitude, in spite of the large discrepancies in the atmospheric masses. The possibility of providing constraints to the 3D dynamics of the fluid envelope based only upon 2D observations of radiative fluxes seems promising for the observational study of planets and for testing numerical models.

1. Introduction

It has long been recognized that adopting a thermodynamical perspective, as pioneered by Lorenz (1955, 1967), may prove of great utility for providing a satisfactory theory of climate dynamics able to tackle simultaneously balances of physical quantities and dynamical instabilities, and aimed at explaining the global structural properties of the climate system, as envisaged by Saltzman (2002). This is of great relevance in terms of the pursuit for explaining climate variability and change on a large variety of scales, covering major paleoclimatic shifts, almost regularly repeated events such as ice ages, as well as the ongoing and future anthropogenic climate change. Additionally, this strategy may prove of great relevance for the provision of reliable metrics for the validation of climate models, as asked for by the Intergovernmental Panel on Climate Change (IPCC 2007) and discussed, e.g., in Held (2005), Lucarini (2008a). See Lucarini and Ragone (2010) for a recent example.

Along the lines of non-equilibrium macroscopic thermodynamics (Prigogine 1962, De Groot and Mazur 1984), the climate can be seen as a non-equilibrium system, which transforms potential into mechanical energy like a thermal engine and generates entropy by irreversible processes. When the external and internal parameters have fixed values, the climate system achieves a steady state by balancing the thermodynamical fluxes with the surrounding environment (Peixoto and Oort 1992).

The concept of the energy cycle of the atmosphere introduced by Lorenz (1955, 1967) allowed for defining an effective climate machine such that the atmospheric and oceanic motions simultaneously result from the mechanical work (then dissipated in a turbulent cascade) produced by the engine, and re-equilibrate the energy balance of the climate system (Stone 1978a,b, Barry et al. 2002). Johnson (2000) introduced a Carnot engine–equivalent picture of the climate system by defining effective warm and the cold reservoirs and their temperatures. Recently, Tailleux (2009)

proposed a fresh outlook on the energetics of the ocean circulation along similar lines.

The interest towards studying the climate irreversibility largely stems from the proposal of the maximum entropy production principle (MEPP) by Paltridge (1975), which suggests that the climate is a non-equilibrium nonlinear systems adjusting in such a way to maximize the entropy production (Grassl 1981, Mobbs 1982, Kleidon and Lorenz 2005). The MEPP has found applications and has raised interest in a large variety of scientific fields (Martyushev and Seleznev 2006). Even if recent claims of *ab-initio* derivation of MEPP (Dewar 2005) have been dismissed (Grinstein and Linsker 2007), strong criticisms have arisen within the geophysical community (Goody 2007), and, recently, the relevance of the boundary conditions of the analysed system has been underlined (Li 2009), this principle has stimulated the re-examination of entropy production in the climate system (Peixoto et al. 1991, Peixoto and Oort 1992, Goody 2000, Fraedrich and Lunkeit 2008, Pascale et al. 2009) and the development of new strategies for improving the parameterisations of climate models (Kleidon et al. 2006). Moreover, a more detailed analysis of the various processes responsible for the entropy production has lead to clarifying the relative role of contributions due to radiative processes, mainly related to the degradation of the photons exergy by the thermalisation of the solar radiation at terrestrial temperatures (Wu and Liu 2009), and those due to the turbulent processes related to the motions of the fluid envelope of the planet (Goody 2000). The latter contributions, which add up to the so-called material entropy production, albeit relatively small, are expected to be of greater relevance as diagnostics of the large scale properties of the system (Ozawa et al. 2003, Lucarini 2009).

In recent years, a great effort has been devoted to improving the thermodynamical description of the climate system by taking into account in a more profound way the irreversible processes associated with the mixing and phase changes of water vapour (Goody 2000, Pauluis 2000, Pauluis and Held 2002a,b, Romps 2008). Whilst these theoretical contributions are crucial for assessing with a

higher degree of precision the components of the entropy budget of the climate system, we shall see that a simpler and more manageable description of the climate thermodynamics has excellent performances for estimating the material entropy production of the system.

We should note that when the material entropy production of the climate system is analysed, most of the attention is devoted to atmospheric processes, with the ocean being of relevance only as boundary conditions with a role not qualitatively different from that of land surface. While being of great relevance when the energetics of the climate system is considered, the contribution to the material entropy production resulting from ocean processes is indeed negligible (Shinokawa and Ozawa 2001), basically because, apart from the mixed layer, the world ocean is up to a good approximation an isothermal fluid. The oceanic entropy production is found to be less than 2% of the atmospheric one (Pascale et al. 2009). Shinokawa and Ozawa (2001), in an analysis that mirrors the investigations on atmospheric thermodynamics discussed above (Goody 2000, Pauluis 2000, Pauluis and Held 2002a,b, Romps 2008), also specifically analysed the entropy production due to the irreversible mixing of salt in the ocean waters, concluding that it is about three orders of magnitude smaller than the contributions due to heat transport.

Recently, a link has been found between the Carnot efficiency, the intensity of the Lorenz energy cycle, the material entropy production and the degree of irreversibility of the climate system (Lucarini 2009). Namely, the efficiency of the equivalent thermal machine sets also the proportionality between the internal entropy fluctuation of the system and the lower bound to entropy production by the fluid compatible with the 2^{nd} law of thermodynamics. Such a bound is basically given by the entropy produced by the dissipation of the mechanical energy, whereas the excess of entropy production is due to the turbulent transport of heat down the gradient the temperature field.

These results have paved the way for a new, extensive exploration aimed at understanding the

climate response under various scenarios of forcings, of atmospheric composition, and of boundary conditions. Recent preliminary efforts using PLASIM (Fraedrich et al. 2005), a simplified yet Earth-like climate model, have focused on the impacts on the thermodynamics of the climate system of changes in the solar constant, with the analysis of the onset and decay of snowball Earth conditions (Lucarini et al. 2010a), and on those due to changing CO_2 concentration (Lucarini et al. 2010b). The former paper has shown how the changeovers between ice-covered and ice-free planet are related to radical changes in the thermodynamics of the climate system, with spontaneous climate transitions accompanying a reduction in the efficiency of the climate machine, and the consequent attainment of a state closer to equilibrium. The latter paper has instead emphasized the importance of framing correctly the hydrological cycle for understanding correctly climate change, as increases in the latent heat transports fuelled by the temperature-driven exponential growth of amount of water vapour in the atmosphere impact very strongly both the efficiency and the degree of irreversibility of the system. These results could also be applied for studying the *climates* of celestial bodies such as extraterrestrial planets and satellites. This is a rather promising and exciting perspective, given the ever increasing attention paid to, and data obtained on, these astronomical objects. It is encouraging that various models belonging to the PLASIM family have already been adapted to study the atmospheres of Titan (Grieger et al. 2004) and Mars (Stenzel at al. 2007). Earlier studies on the MEPP have also tackled this point (Lorenz et al. 2001, Ozawa et al. 2003).

A potentially serious problem when performing a complete analysis of the planetary system in terms of the 2nd law of thermodynamics, which boils down to computing the material entropy generation, the Carnot efficiency, and the degree of irreversibility of the system is that three dimensional, time dependent information on the intensive thermodynamical quantities, of their tendencies, and of the forcing terms are required (Lucarini 2009). It has been proved that for a given

numerical model constructing the suitable diagnostic tools is feasible and definitely not computationally burdensome, as only integral operators (which boil down to weighted sums) are involved (Fraedrich and Lunkeit 2008). Moreover, when computing climatological averages of the thermodynamical properties, using time averaged fields (e.g. annual means) as opposed to instantaneous one does not introduce large biases, even if nonlinear quantities are involved, since short-time scale covariability of the involved fields results to be not very relevant (Lucarini 2009).

On the other side, deducing the thermodynamics of the system from observations is a rather complex matter, since it is hard to obtain accurate reconstructions of all the involved 3D thermodynamic quantities with sufficient resolution. This problem is especially delicate when applications to planets other than the Earth, and especially those not belonging to the Solar system, are considered. In most cases, we can rely on remote sensing observational techniques, which provide, at the most basic level, information on the 2D fields of "hot" incoming stellar radiation and of outgoing radiation emitted at lower temperature by the planet and surely cannot tell us everything we need on the internal structure of the planet.

In this paper we introduce an approximate formula which allows for splitting the material entropy production into two contributions, one related to horizontal, planetary scale transport processes, the other one related to vertical processes. The two contributions can be computed separately using 2D radiative fields at the top of the atmosphere (TOA) and at surface. We focus our attention on Earth-like conditions, but the approach can also be used to analyse general planetary systems. The contribution to the material entropy production due to horizontal processes can be computed using 2D radiative fields at the top of the atmosphere only, so that it is of easier access for a larger class of planetary objects. Such estimate allows for computing a lower bound to the total values of material entropy production and intensity of the Lorenz energy cycle, or, equivalently, of the

average rate of total dissipation of the kinetic energy. Moreover, by combining energy and entropy constraints, it is possible to provide insights on a previous intuition on the possibility of defining a baroclinic heat engine extracting work from the meridional heat flux (Barry et al. 2002). The proposed bounds translate into approximate identities if we can assume a vertically quasi-isothermal temperature structure. We first test our theoretical findings by comparing the result of our approximate formulas with detailed calculations presented in the literature. We then take advantage of our approach to analyse the thermodynamic properties of the pre-industrial (PI) control runs of the CMs included in the PCMDI/CMIP3 dataset, thus extending the results of Lucarini and Ragone (2010) to the "2nd law of thermodynamics" diagnostics. We take into account first and second moments of thermodynamical quantities describing out-of-equilibrium properties, in order to assess their climatology and their (co-)variability, thus testing equilibration processes. Finally, in order to test the relevance of our approach in conditions where only the radiation fields at the top of the atmosphere can be measured, we apply our findings to observational data and obtain some relevant new results on the thermodynamic properties of the Earth, Mars, Titan and Venus' climates.

The paper is divided as follows. In Section 2 we review two distinct formulas allowing for evaluating the material entropy production of a generic planetary system and perform a suitable scale analysis. In section 3 we show how to derive the above described approximate formulas and general bounds on the material entropy production and on parameters describing the degree of irreversibility of the system. We also discuss the relevance of simple 2-box models (Kleidon and Lorenz 2005), usually adopted for describing the basic features of entropy production and explain why they miss fundamental (and quantitatively dominant) ingredients. We propose that four in the minimum number of boxes needed for achieving a conceptually correct description of entropy production in a planetary system. In Section 4 we verify the validity of the approximate formula and exploit it to

estimate the thermodynamical properties of the CMs included in the PCMDI/CMIP3 dataset in preindustrial climate conditions. In section 5 we present specific results for the bounds to the material entropy production and intensity of the Lorenz energy cycle for Earth, Mars, Titan and Venus. In section 6 we present our conclusions and perspectives for future work.

2. Rate of Material Entropy Production

2.1 Theoretical Outlook

The traditional approach for the investigation of the entropy production of the climate system relies on separating the contributions due to irreversible processes involving matter and those due to irreversible changes in the spectral properties of the radiation.

The process of thermalisation of the solar radiation gives by far the most important contribution to the global planetary entropy production, basically as it involves the transformation of electromagnetic energy travelling through space obeying a Planckian spectrum with the temperature signature of the Sun's corona (about 5800 K) into (quantitatively identical) electromagnetic energy whose spectral properties are approximately described by a Planckian spectrum at the Earth's emission temperature (about 250 K). A very detailed and extensive account of these processes and their contribution in terms of entropy production has recently been given by Wu and Liu (2009).

The rest of the irreversible processes taking place in the climate system provide a much smaller contribution to the entropy production, basically because much less relevant temperature (or chemical potential) differences are involved. The irreversible transformations occurring in the climate systems involve in principle a great variety of phenomena, including dissipation of mechanical energy, heat transport down the temperature gradient, irreversible mixing and phase transitions.

In a system at steady state, the expectation value of the extensive, integrated material entropy does not depend on time. Following (Johnson 2000; Goody 2000), it is possible to derive the following equation for the total entropy *S* of the climate system:

$$\overline{\dot{S}} = \int_{\Omega} dV \left(\overline{\frac{\dot{q}_{rad}}{T}} + \overline{\dot{s}_{turb}} \right) = 0 \,. \qquad (1)$$

where Ω is the spatial domain of integration, the dot indicates the operation of time derivative, the overbar indicates the operation of long term average, *T* is the local temperature of the medium, $\dot{q}_{rad}$ is the heating due to the convergence of the radiation fluxes, while $\dot{s}_{turb}$ is the density of entropy production due to irreversible processes involving the fluid medium, and is usually referred to as local material entropy production (Ozawa et al. 2003). Therefore, we obtain:

$$\overline{\dot{S}_{mat}} = \int_{\Omega} dV \, \overline{\dot{s}_{turb}} = -\int_{\Omega} dV \, \overline{\frac{\dot{q}_{rad}}{T}} \qquad (2)$$

where $\overline{\dot{S}_{mat}}$ is the average rate of material entropy production of the climate system. This equation provides us with two recipes for computing the material entropy production, one based on the direct computation of the spatial integral of $\dot{s}_{turb}$, and the other (the "inverse formula") based on the evaluation of the interaction between radiation and matter. Depending on the degree of detail and precision we adopt in the representation of the physicochemical properties of the climate system, we may derive different expressions for $\dot{s}_{turb}$, which are suited for characterizing a wider or smaller

number of irreversible processes.

At the lowest level of such a hierarchy, one assumes the fluid medium of the planet as homogenous, where a monophase fluid “dry air” and a monophase “sea water” are considered and phase changes and mixing processes occurring in the atmosphere and in the ocean are altogether neglected. In this case, the local material entropy production can be expressed as:

$$\dot{s}_{turb} = \frac{\varepsilon^2}{T} + \vec{F}_{SH} \cdot \vec{\nabla} \frac{1}{T}, \tag{3}$$

where the two contributions to entropy production are given by dissipation ε^2 of kinetic energy (first term) and by the component of sensible heat flux $\vec{F}_{SH}$ down the temperature gradient performed by turbulent fluxes (second term). Such a model is manifestly insufficient for describing multi-phase systems like the Earth System in present conditions, as latent heat fluxes are largely dominant over sensible heat fluxes (Peixoto and Oort 1992). The easiest way to account for water phase changes in the material entropy budget relies on expressing $\dot{s}_{turb}$ as follows:

$$\dot{s}_{turb} = \frac{\varepsilon^2}{T} + \vec{F}_{SH} \cdot \vec{\nabla} \frac{1}{T} + \vec{F}_{LH} \cdot \vec{\nabla} \frac{1}{T}, \tag{4}$$

where ε^2 includes also the dissipation of kinetic energy due to the friction of the falling hydrometeors and $\vec{F}_{LH}$ is the flux of latent heat. Such a formula has been widely used for estimating the entropy production of the Earth system (Peixoto et al 1991, Peixoto and Oort 1992, Fraedrich and Lunkeit 2008, Pascale et al. 2009, Lucarini et al. 2010a, 2010b). Note that, in snowball conditions,

where the phase transitions of the water substance are virtually absent due to the extremely cold temperature, the two formulations (3) and (4) are virtually equivalent.

Romps (2008) refers to the representation of the entropy production given by Eq. (4) as resulting from a “dry” description of a “moist” atmosphere, because water is treated mainly as a passive substance, while processes such as irreversible mixing of the water vapour is altogether ignored. More detailed, “moist” descriptions of a “moist” atmosphere have led to formulations of atmospheric thermodynamics able to account for these processes (Goody 2000, Pauluis 2000, Pauluis and Held 2002a,b, Romps 2008). It is useful to remind that additional contributions to the entropy production are given by the irreversible mixing of salt in the ocean (Shinokawa and Ozawa 2001). Such more refined formulations of the entropy processes inside the climate system account for a consistent treatment of the entropy generated by the hydrological cycle.

Given the complex nature of the climate system, additional processes contributing to entropy production can be highlighted. Kleidon (2009) presents a complete and holistic account of this issue, suggesting that biological and geochemical processes, as well as the great variety of chemical processes taking place in the atmosphere should in principle be included to get a truly complete treatment of the entropy budget of the Earth system.

Since we aim at a parsimonious but efficient representation of the entropy production of the of the climate system science, we would like to be able to choose an approach, which translates into an explicit expression for $\dot{s}_{turb}$, which is as simple as possible but, at the same time, provides a good approximation to the entropy production.

The volume integration of $-\overline{\dot{q}_{rad}/T}$ gives the exact value of the entropy production, so that the indirect approach allows on one side to obtain precise estimates, and on the other side to test the

validity of different explicit formulations for $\dot{s}_{turb}$ and, consequently, of the level of detail we adopt in describing the climatic thermodynamic processes. Interpreting previous climate models' results is definitely useful in this direction. Pascale et al. (2009), who considered two fully coupled atmosphere-ocean climate models, clearly showed that in present day conditions the identity given by equation (2) is obeyed up to an excellent degree of precision when we use for $\dot{s}_{turb}$ the expression given in Eq. (4). The observed agreement is within 1% and of the same order of magnitude of the uncertainty in the material entropy production due to the bias in the imperfect closure of the energy cycle due to spurious energy sinks/sources inside the system (Lucarini et al. 2010a,b; Lucarini and Ragone 2010). Already Goody (2000) observed that adopting a more detailed physical description of the atmosphere where irreversible water vapour mixing processes are considered changes only slightly the estimate of the material entropy production. We may then conclude that whereas the sophisticated thermodynamical framework developed in (Pauluis 2000, Pauluis and Held 2002a,b, Romps 2008) is crucial for understanding in detail the various terms contributing to the entropy budget of the climate system, the simpler formulation (Peixoto et al 1991, Peixoto and Oort 1992, Fraedrich and Lunkeit 2008, Pascale et al. 2009, Lucarini et al. 2010a, 2010b) provides rather accurate results when only the material entropy production is taken into account.

Note also that in planetary systems other than the Earth, turbulent fluxes related to phase transitions which are different from those relevant for the hydrological cycle can be relevant (e.g. CO_2 sublimation on Mars), so that Eq. (4) has to be changed accordingly.

2.2 Scale Analysis: Direct Expression of Entropy Production

The "direct" expression for the material entropy production is considered first. Using Gauss' theorem, we can write:

$$\overline{\dot{S}_{mat}} = \int_{\Omega} \overline{\frac{\varepsilon^2}{T}} dV + \int_{\Omega} \overline{\vec{F} \cdot \vec{\nabla} \frac{1}{T}} dV = \int_{\Omega} \overline{\frac{\varepsilon^2}{T}} dV + \int_{\Omega} \overline{\vec{\nabla} \cdot \left(\frac{\vec{F}}{T} \right)} dV - \int_{\Omega} \overline{\left(\frac{\vec{\nabla} \cdot \vec{F}}{T} \right)} dV =$$

$$= \int_{\Omega} \overline{\frac{\varepsilon^2}{T}} dV + \int_{\partial\Omega} \overline{\hat{n} \cdot \left(\frac{\vec{F}}{T} \right)} d\sigma - \int_{\Omega} \overline{\left(\frac{\vec{\nabla} \cdot \vec{F}}{T} \right)} dV = \int_{\Omega} \overline{\frac{\varepsilon^2}{T}} dV - \int_{\Omega} \overline{\left(\frac{\vec{\nabla} \cdot \vec{F}}{T} \right)} dV . \qquad (5)$$

As discussed in Lucarini (2009), the volume integral of the first term on the right hand side of Eq. (5) basically gives us the lower bound to the entropy production compatible with the system having a global mean dissipation of kinetic energy (and production of mechanical work) equal to $\overline{W} = \overline{D} = \int \overline{\varepsilon^2} dV$. The second term in Eq. (5) vanishes as no material fluxes are present at the top of the atmosphere. Turbulent transport occurs mainly in the vertical direction (Peixoto and Oort 1992), so that $\vec{\nabla} \cdot \vec{F} \approx \partial_z F_z$. The material flux $\vec{F}$ accounts for both the sensible and heat turbulent heat fluxes, so that $\vec{F} = \vec{F}_{SH} + \vec{F}_{LH}$. The two fluxes have rather different properties since sensible heat turbulent transport is mostly relevant for the interaction between the surface and the boundary layer of the atmosphere, whereas the latent heat turbulent flux is such (on our planet) that it picks up water vapour at unsaturated, relatively warm surface conditions and transports it to regions with lower temperatures where condensation and precipitation occur. A similar scenario can be envisaged also for other planets, where different phase transitions could be involved. Extending the approach by Fraedrich and Lunkeit (2008), we can rewrite Eq. (5) in a simpler 2D form as:

$$\overline{\dot{S}_{mat}} = \int_{A} \frac{\left\langle \varepsilon^2 \right\rangle}{T_{diss}} d\sigma + \int_{A} \left(\frac{1}{T_{SH}^{+}} - \frac{1}{T_{SH}^{-}} \right) \overline{F_{z,S}^{SH}} d\sigma + \int_{A} \left(\frac{1}{T_{LH}^{+}} - \frac{1}{T_{LH}^{-}} \right) \overline{F_{z,S}^{LH}} d\sigma \qquad (6)$$

$$= \overline{\dot{S}_{mat}^{diss}} + \overline{\dot{S}_{mat}^{SH}} + \overline{\dot{S}_{mat}^{LH}}$$

where $\overline{F_{z,S}^{SH}}$ and $\overline{F_{z,S}^{LH}}$ are the long term averages of the sensible and latent heat fluxes at the surface, T_{diss} is a suitably time averaged 2D field of characteristic temperature for kinetic energy dissipation ($T_{diss} = \int \overline{\varepsilon^2} dz \Big/ \int \overline{\varepsilon^2 / T} dz$, with $\int \overline{\varepsilon^2} dz = \left\langle \overline{\varepsilon^2} \right\rangle$). For each column of fluid, we can define the following characteristic temperatures for the sensible and leant heat exchange processes. T_{SH}^{+} and T_{LH}^{+} are the characteristic 2D fields of temperatures at which sensible and latent heat are removed, while T_{SH}^{-} and T_{LH}^{-} are the 2D fields of characteristic temperatures at which sensible and latent heat are absorbed. Formally, this is achieved by dividing each column into two domains in the z-direction, one where $\partial_z F_z$ is positive, and one where $\partial_z F_z$ is negative. The two temperatures are then defined similarly to T_{diss} described above where the vertical is performed only over the domain with the corresponding sign for $\partial_z F_z$ and values are weighted according to the value of $\partial_z F_z$. Note that this operation is performed separately for the latent and sensible heat flux. This approach is similar to the *net exchange formulation* proposed by Green (1967) to study radiative transfer proposed (see also below). As inside the ocean the gradients of sensible heat fluxes are very weak (and gradients of latent heat fluxes do not make any sense), the atmosphere and its lower interface (solid or liquid) only contribute to Eq. (6). As in each column most of the sensible and latent heat is removed at or very close to surface, we assume $T_{SH}^{+} \approx T_{LH}^{+} \approx T_S$. Instead, we expect that T_{SH}^{-} is closely approximated by the temperature of the boundary layer T_{BL}, while we indicate T_{LH}^{-} with T_C, since it refers to the average condensation temperature.

Since the turbulent transport of sensible heat is an eminently local process, its contribution $\overline{\dot{S}_{mat}^{SH}}$ to the material entropy production is not very large. Instead, the contribution to the material

entropy production coming from latent heat ($\overline{\dot{S}_{mat}^{LH}}$) is largely dominant, and involves evaporation, condensation, and transport processes occurring in the context of the hydrological cycle (see also Pascale et al. 2009).

Note that it is possible to define the degree of irreversibility of the system (Lucarini 2009) by introducing the parameter $\alpha = \left(\overline{\dot{S}_{mat}^{SH}} + \overline{\dot{S}_{mat}^{LH}}\right) \Big/ \overline{\dot{S}_{mat}^{diss}}$ where symbols refer to Eq. (6). The parameter α is conceptually equivalent to the Bejan number (Paoletti et al. 1989), which is a commonly studied parameter when the performances of engineering systems are considered. When α=0 (and the Bejan number, which can be expressed as α+1, is unity), the system features the smallest rate of material entropy production compatible with the presence of a Lorenz energy cycle of intensity $\overline{W} = \overline{D} = \int \overline{\varepsilon^2} dV$. If α=0, all the entropy is generated via dissipation of kinetic energy, with no contributions coming from fluxes transporting heat down the gradient of the temperature. Recent model simulations have shown that warmer climate conditions trigger a fast increase in the degree of irreversibility of the Earth system, the main reason being the large sensitivity of latent heat fluxes to increases in the atmospheric and surface temperature (Lucarini et al. 2010a, 2010b).

In Eq. (6), along the lines of what happens on Earth, we consider just one dominant phase transition as relevant for entropy generation. In other planets, we may need to add other terms on the right hand side (with distinct characteristic temperatures) to account for various phase transitions.

2.3 Scale Analysis: Indirect Expression of Entropy Production

The “indirect” expression for the material entropy production is considered now. We emphasize that such an approach bypasses the problems related to the details in the representation of the atmospheric processes discussed at the beginning of this section. The solar shortwave (SW) radiation

heats the system, whereas the infrared longwave (LW) radiation acts as a net cooler. Moreover, we split processes occurring within the atmosphere from those occurring at surface, which we interpret as boundary between the gaseous medium and the solid and liquid medium, thus moving along the lines of the *net exchange formulation* (Green 1967). Along the same lines followed to derive Eq. (6), we write the average rate of material entropy production as follows:

$$\overline{\dot{S}_{mat}} = -\int_A \frac{\overline{SW_{surf}} + \overline{LW_{surf}}}{T_S} d\sigma - \int_A \frac{\overline{SW_{TOA}} - \overline{SW_{surf}}}{T_{A,SW}} d\sigma - \int_A \frac{\overline{LW_{TOA}} - \overline{LW_{surf}}}{T_{A,LW}} d\sigma , \qquad (7)$$

where $\overline{SW_{surf}}$ and $\overline{LW_{surf}}$ are the average fluxes of SW and LW radiation at surface, $\overline{SW_{TOA}}$ and $\overline{LW_{TOA}}$ are the average fluxes of SW and LW radiation at the top of the atmosphere. Similarly to what discussed in the previous subsection, $T_{A,SW}$ and $T_{A,LW}$ represent the 2D fields of characteristic atmospheric temperatures at which absorption of SW and LW, respectively, occur. On our planet, most of the SW is absorbed at surface or in the first few meters of ocean, so that the atmosphere is heated from below. This applies for all planets whose atmosphere is approximately transparent to SW radiation. We may rewrite Eq. (7) as follows:

$$\overline{\dot{S}_{mat}} = -\int_A \overline{SW_{surf}} \left(\frac{1}{T_S} - \frac{1}{T_{A,SW}} \right) d\sigma - \int_A \overline{LW_{surf}} \left(\frac{1}{T_S} - \frac{1}{T_{A,LW}} \right) d\sigma - \int_A \frac{\overline{SW_{TOA}}}{T_{A,SW}} d\sigma - \int_A \frac{\overline{LW_{TOA}}}{T_{A,LW}} d\sigma . \qquad (8)$$

We now assume – on a heuristic basis – that $T_{A,SW} \approx T_{A,LW} \approx T_E = \sqrt[4]{\overline{LW_{TOA}}/\sigma}$, where T_E is the 2D field of the emission temperature of the planet. This means that the vertically averaged characteristic

temperature of *atmospheric* absorption and emission are similar. We then obtain:

$$\overline{\dot{S}_{mat}} \approx -\int_A \left(\overline{SW_{surf}} + \overline{LW_{surf}}\right)\left(\frac{1}{T_S} - \frac{1}{T_E}\right)d\sigma - \int_A \frac{\left(\overline{SW_{TOA}} + \overline{LW_{TOA}}\right)}{T_E}d\sigma$$

$$\approx -\int_A \left(\overline{SW_{surf}} + \overline{LW_{surf}}\right)\left(\frac{1}{T_S} - \frac{1}{T_E}\right)d\sigma - \int_A \frac{\vec{\nabla}_H \cdot \overline{\vec{H}}}{T_E}d\sigma$$

$$\approx \overline{\dot{S}_{mat}^{vert}} + \overline{\dot{S}_{mat}^{hor}}, \qquad (9)$$

where in the last passage we have used that the convergence of large scale, non-turbulent reversible enthalpy horizontal transport $\vec{H}$ balances the net radiative budget at the top of the atmosphere when long term averages are considered (Peixoto and Oort 1992, Lucarini and Ragone 2010). Equation (9) tells us that the material entropy production can be, alternatively to the splitting proposed in Eq. (6), conceptually decomposed into two terms. The term $\overline{\dot{S}_{mat}^{vert}}$ describes the vertical transport of radiation between two reservoirs, one at the surface temperature, the other one at temperature of the bulk of the atmosphere, and is closely related to dry and moist convective processes (Emanuel 2000). This term treats the fluid envelope as a collection of independent vertical columns dominated by fast exchanges and interactions. The term $\overline{\dot{S}_{mat}^{hor}}$ describes the effect of horizontally transporting energy in a 2D fluid system with spatially varying temperature structure, and is associated to longer time scales. Both terms are positive, the first because the atmosphere is on the average colder than the underlying surface, as the system is heated from below, the second because temperature is lower where there is convergence of enthalpy fluxes, and larger where divergence is observed, in agreement with the second law of thermodynamics (Peixoto and Oort 1992, Ambaum

2010). The two spatial fields whose integrals give $\overline{\dot{S}_{mat}^{hor}}$ and $\overline{\dot{S}_{mat}^{vert}}$ are expected to have different properties, as the former should be positive everywhere, because each column is described as a quasi-isolated system producing entropy, whereas the sign of the latter will depend on the sign of the radiative budget at TOA.

Note that a discretised version of the second term in Eq. (9), based upon a 2-box approximation of the fluid envelope of the climate system, has been considered as proxy for the total material entropy production (Lorenz et al. 2001, Kleidon 2009). Instead, from Eq. (9) it is apparent that a minimal model of the whole material entropy production of a planetary system must include, in addition to the box of the warm (Box 1) and cold (Box 2) portions of the fluid envelope of the planet, two additional boxes, each representing the planetary surface in the warm (Box 3) and cold (Box 4) regions of the planet. See Fig. 1 for a conceptual scheme, where the arrows indicate the couplings defining the time evolution of the system. Note that the ocean has a dual role: on one side, it acts a lower surface exchanging with the atmosphere sensible and latent heat fluxes (as done by the land surface), on the other side, it has the dynamic role of contributing, as part of the fluid envelope of the planet, to the transport of heat from the warm to the cold box. Note that the internal oceanic processes have only a minor relevance in terms of entropy production (Pascale et al. 2009).

3. Bounds to the Thermodynamical Properties of a Planetary System

Since $T_{BL} \approx T_S$, we have that $T_{BL} > T_E$. Since the water vapour saturation mixing ratio strongly increases with temperature, and since on Earth the atmospheric temperature decreases with height, the vertical scale of water vapour in globally saturated conditions is smaller than that of the atmosphere. The situation is altered as the atmosphere is not saturated, so that we can assume

$T_C \approx T_E$ (Peixoto and Oort 1992). As the temperature dependence of saturation mixing ratio is analogous for general phase transitions, as the non-gaseous reservoirs are mostly located at surface, and as the temperature decreases with height if a planet is heated from below, we expect that $T_C \approx T_E$ is a reasonable assumption for general phase transitions on a generic planet. Using Eq. (6), we obtain:

$$\overline{\dot{S}_{mat}} < \int_A \frac{\overline{\varepsilon^2}}{T_{diss}} d\sigma + \int_A \left(\overline{F_{z,surf}^{SH}} + \overline{F_{z,surf}^{LH}} \right) \left(\frac{1}{T_S} - \frac{1}{T_E} \right) d\sigma \qquad (10)$$

Since at surface energy balance applies, we have that $\overline{SW_{surf}} + \overline{LW_{surf}} + \overline{F_{z,surf}^{SH}} + \overline{F_{z,surf}^{LH}} = \vec{\nabla} \cdot \overline{\vec{H}_{surf}}$, where $\vec{\nabla} \cdot \overline{\vec{H}_{surf}}$ is the divergence of the transport performed by the liquid portion of the fluid envelope, i.e., in the Earth case, by the ocean. If a planet has a negligible amount of liquid medium, this term can be set to zero. By comparing Eqs. (9) and (10), we obtain that the material entropy production by dissipation of kinetic energy is bounded from below by the entropy produced by the large scale horizontal transport of heat:

$$\int_A \frac{\overline{\varepsilon^2}}{T_{diss}} d\sigma > -\int_A \frac{\vec{\nabla}_H \cdot \overline{\vec{H}}}{T_E} d\sigma - \int_A \vec{\nabla}_H \cdot \overline{\vec{H}_{surf}} \left(\frac{1}{T_S} - \frac{1}{T_E} \right) d\sigma \approx -\int_A \frac{\vec{\nabla}_H \cdot \overline{\vec{H}}}{T_E} d\sigma \Rightarrow \overline{\dot{S}_{mat}^{diss}} > \overline{\dot{S}_{mat}^{hor}} . \qquad (11)$$

The second term in the first inequality in expression (11) can be surely neglected if no liquid medium is present on the planet. Moreover, under the reasonable hypothesis that $\left(1/T_S - 1/T_E\right)$ is approximately constant (roughly corresponding to a spatially homogeneous atmospheric lapse rate),

the term is also negligible, since the area integral of the horizontal convergence of subsurface enthalpy flux vanishes. Even with a more conservative scale analysis, we basically obtain the same result, because $\left|1/T_E\right| >> \left|1/T_S - 1/T_E\right| = \left|1/T_E\right| \times \left|\left(T_E - T_S\right)/T_S\right|$ and, in the case of Earth, the ocean enthalpy transport contributes to only about 30% of the total enthalpy transport (Lucarini and Ragone 2010). We conclude that Eq. (11) tells us that the material entropy production by dissipation of kinetic energy is bounded from below by the entropy produced by the horizontal transport of heat performed by the large scale motion.

Equation (11) allows us to derive an approximate inequality providing a constraint on the intensity of the Lorenz energy cycle $\overline{W} = \overline{D} = \int \overline{\varepsilon^2} dV$. As half of the kinetic energy is dissipated mainly at the boundary layer and half in the free atmosphere (Peixoto and Oort 1992), we have $T_E \le T_{diss} \le T_{BL} \approx T_S$. Since $\overline{\varepsilon^2}$ is positive definite and the fractional spatial variation of T_S is relatively small, we derive:

$$\overline{W} = \overline{D} = \int_A \overline{\varepsilon^2} d\sigma \ge -\left\langle T_S \right\rangle \int_A \frac{\vec{\nabla}_H \cdot \overline{\vec{H}}}{T_E} d\sigma \ge -\left\langle T_E \right\rangle \int_A \frac{\vec{\nabla}_H \cdot \overline{\vec{H}}}{T_E} d\sigma = \left\langle T_E \right\rangle \overline{\dot{S}^{hor}_{mat}} \tag{12}$$

where the square brackets indicate spatial averaging, and the last inequality derive from the fact that $\left\langle T_S \right\rangle \ge \left\langle T_E \right\rangle$. Note that the safer inequality:

$$\overline{W} \ge -\left\langle T_E \right\rangle \int_A \frac{\vec{\nabla}_H \cdot \vec{H}}{T_E} d\sigma = -\left\langle T_E \right\rangle \int_A \frac{\overline{R}}{T_E} d\sigma = \overline{W}_{\min} = \left\langle T_E \right\rangle \overline{\dot{S}^{hor}_{mat}}, \tag{13}$$

where $\overline{SW_{TOA}} + \overline{LW_{TOA}} = \overline{R}$, allows us to put a constraint on the intensity of the Lorenz energy cycle and on the corresponding rate of dissipation of the kinetic energy purely on quantities that can be derived from measurements (or model data) evaluated at the top of the atmosphere. If the planet has no atmosphere, so that $\overline{W} = 0$, the right term of the inequality must also be vanishing. This is consistent with the fact that in the absence of a fluid envelope, no enthalpy can be transported horizontally, so that when long term averages area considered, $\vec{\nabla}_H \cdot \overline{\vec{H}} = \overline{SW_{TOA}} + \overline{LW_{TOA}} = \overline{R} = 0$. This implies that the SW and LW fluxes at the top of the (infinitesimal) atmosphere have to be everywhere equal in magnitude and opposite in sign.

3.1 Baroclinic Efficiency

We can rewrite Eq. (13) as follows:

$$\overline{W} \geq \overline{W_{\min}} = -\langle T_E \rangle \left(\int_{A_>} \frac{\overline{R}}{T_E} d\sigma + \int_{A_<} \frac{\overline{R}}{T_E} d\sigma \right), \tag{14}$$

where we have divided the domain in two regions $A_>$ and $A_<$, the former (latter) describing the subdomain featuring a positive (negative) radiation budget at the top of the atmosphere. We can express Eq. (14) as:

$$\overline{W} \geq \overline{W_{\min}} = -\langle T_E \rangle \left(\frac{\langle \overline{R} \rangle_> |A_>|}{T_E^>} + \frac{\langle \overline{R} \rangle_< |A_<|}{T_E^<} \right), \tag{15}$$

where $\langle R \rangle_{>}$ is the spatial average of the net radiative budget performed on the 2D domain $A_{>}$ (having measure $|A_{>}|$), with equivalent notation applying for the negative radiative balance case. Note that $|A_{>}| + |A_{<}| = |A|$. Since $\int_A \overline{R} d\sigma = 0$, so we have that $\langle \overline{R} \rangle_{>} |A_{>}| + \langle \overline{R} \rangle_{<} |A_{<}| = 0$. Instead, $T_E^{>}$ and $T_E^{<}$ are reference temperatures obtained by averaging the emission temperature over the domains $A_{>}$ and $A_{<}$, respectively, and using the value of the net radiative budget as weighting function:

$$T_E^{>(<)} = \frac{\int_{A_{>(<)}} \overline{R} d\sigma}{\int_{A_{>(<)}} \frac{\overline{R}}{T_E} d\sigma}. \qquad (16)$$

We then obtain:

$$\overline{W} \geq \overline{W_{\min}} = \langle \overline{R} \rangle_{>} |A_{>}| \langle T_E \rangle \left(\frac{1}{T_E^{<}} - \frac{1}{T_E^{>}} \right) = \eta_h \langle \overline{R} \rangle_{>} |A_{>}|, \qquad (17)$$

with

$$\eta_h = \langle T_E \rangle \left(\frac{1}{T_E^{<}} - \frac{1}{T_E^{>}} \right) \approx \frac{T_E^{>} - T_E^{<}}{\langle T_E \rangle} \approx \frac{T_E^{>} - T_E^{<}}{T_E^{>}} \qquad (18)$$

where we have assumed that $\langle T_E \rangle \approx 1/2 \left(T_E^{>} + T_E^{<} \right)$ and that $\left(T_E^{>} - T_E^{<} \right) / \langle T_E \rangle << 1$. Whereas the first assumption is quite obvious, since we are averaging over two regions $A_{>}$ and $A_{<}$ of analogous size,

we underline that the second assumption is usually verified even in the presence of large spatial variability of the radiative balance, as a fourth root is involved in the definition of the emission temperature. The quantity η_h links the input of radiative energy at an average rate $\left\langle \overline{R} \right\rangle_{>} |A_{>}|$ into the warm subdomain at temperature $T_E^{>}$ to the lower bound to average rate of production of mechanical work , and can be interpreted as the climate Carnot-like efficiency related *only* to differential heating at the top of the atmosphere.

The overall energy balance of the climate system imposes that the fluid envelope of the planet transports through large scale motions an amount of enthalpy $\overline{F} = \left\langle \overline{R} \right\rangle_{>} |A_{>}|$ from the regions of the climate system featuring a positive radiative budget at the top of the atmosphere to those which constantly lose energy to space (Lorenz 1967, Stone 1978b, Peixoto and Oort 1992, Lucarini and Ragone 2010). Due to the fairly zonal nature of the net TOA radiative balance (Peixoto and Oort 1992), such compensation translates into the fact that in each hemisphere the location of the peak of the meridional enthalpy transport coincides with the latitudinal boundary dividing the radiative heated low latitudes and the radiatively cooled high latitudes in the northern (southern) hemisphere. Moreover, since the two hemispheres are rather similar in terms of average zonal energy budgets and inferred meridional transports, as imposed by the constraints given in Stone (1978) and confirmed by Lucarini and Ragone (2010), the intensity of the peak of the transport in either hemisphere is approximately $1/2 \left\langle \overline{R}_{>} \right\rangle |A_{>}|$. The lower bound to the intensity of the Lorenz energy cycle given in Eq. (17) can be interpreted as product of an efficiency related to meridional temperature differences and the fluxes across such meridional gradients. This provides further theoretical insight and suitable conceptual framework to the intuition by Barry et al. (2002) on the possibility of defining a “baroclinic heat engine” extracting work from the meridional heat flux.

What presented here gives the basic ingredients for providing a rigorous construction of the simplified two-box model usually considered in the literature (Lorenz et al. 2001). Such a reduced model, which allows for the description of entropy production due to horizontal processes of heat exchange only, is enclosed in a dashed rectangle in Fig. 1. The warm box (Box 1) is defined by the portion of the fluid envelope of the climate system featuring a positive net radiative balance at TOA and has a temperature equal to $T_E^>$. The cold box (Box 2) is defined by the part of the fluid envelope of the planet featuring a negative net radiative balance at TOA, i.e. the mid-high latitudes, and has temperature equal to $T_E^<$. The irreversible heat transfer $\overline{F} = \left\langle \overline{R} \right\rangle_> \left| A_> \right|$ from warm to cold areas generates entropy at rate:

$$\overline{\dot{S}_{mat}^{hor}} = \left\langle \overline{R} \right\rangle_> \left| A_> \right| \left(1/T_E^< - 1/T_E^> \right) = \eta_h \overline{F} / \left\langle T_E \right\rangle \qquad (19)$$

3.2 Bound on the degree of irreversibility of the system

The bound $\overline{\dot{S}_{mat}^{diss}} > \overline{\dot{S}_{mat}^{hor}}$ obtained in Eq. (11) can be used to introduce a further bound to the thermodynamical properties of the system. With a trivial manipulation of the expression of the parameter of irreversibility α, we obtain:

$$\alpha = \frac{\overline{\dot{S}_{mat}} - \overline{\dot{S}_{mat}^{diss}}}{\overline{\dot{S}_{mat}^{diss}}} < \frac{\overline{\dot{S}_{mat}} - \overline{\dot{S}_{mat}^{hor}}}{\overline{\dot{S}_{mat}^{hor}}} = \frac{\overline{\dot{S}_{mat}^{vert}}}{\overline{\dot{S}_{mat}^{hor}}} = \alpha_{max} \,, \qquad (20)$$

where α_{max} is the upper bound to the parameter of irreversibility. Defining $Be_{max} = \alpha_{max} + 1$ as the upper bound to the Bejan number, one easily obtains that:

$$\frac{Be_{max}}{Be} = \frac{\alpha_{max} + 1}{\alpha + 1} = \frac{\overline{\dot{S}_{mat}}}{\overline{\dot{S}_{mat}^{hor}}} \sim \frac{\overline{W}}{\overline{W_{min}}} \tag{21}$$

so that the product of the lower bound to the intensity of the Lorenz energy cycle and of the upper bound of the Bejan number is equal to the product of the actual Bejan number times the actual intensity of the Lorenz energy cycle.

3.3 Vertically isothermal fluid envelope

If the planet's fluid envelope is approximately isothermal in the vertical direction, we have that the 2D fields $T_E, T_S, T_{diss}, T_{A,LW}, T_{A,SW}, T_C, T_{BL}$ are almost indistinguishable. By applying this to Eqs. (6) and (9), we obtain that inequalities (11)-(13) become approximate identities:

$$\int_A \frac{\overline{\varepsilon^2}}{T_{diss}} d\sigma \approx -\int_A \frac{\vec{\nabla}_H \cdot \overline{\vec{H}}}{T_E} d\sigma \approx -\left(\frac{\left\langle \overline{R} \right\rangle_> |A_>|}{T_E^>} + \frac{\left\langle \overline{R} \right\rangle_< |A_<|}{T_E^<} \right) \tag{22}$$

$$\overline{W} = \int_A \varepsilon^2 d\sigma \approx -\left\langle T_E \right\rangle \int_A \frac{\vec{\nabla}_H \cdot \overline{\vec{H}}}{T_E} d\sigma = \eta_h \left\langle \overline{R} \right\rangle_> |A_>| \tag{23}$$

so that a direct estimate of the average rate of entropy production of the system and of the average intensity of the Lorenz energy cycle can be obtained just by looking at top of the atmosphere radiative budgets. The validity of the estimates (22) and (23) has been confirmed to hold in a recent experiment performed with the HadCM3 coupled climate model where energy fluxes have been arranged consistently in such a way that the vertical derivative of the air temperature is vanishing

(Pascale, private communication, 2010).

In the case of vertically quasi-isothermal fluid only horizontal gradients of heating are relevant for determining generation of available potential energy. Thus, the quantity η_h described in Eq. (18) is expected to agree with the global Carnot climate efficiency η introduced by Johnson (2000), improved by Lucarini (2009), and computed explicitly in climate models in (Lucarini et al., 2010a, 2010b). When the temperature vertical profile is not constant, the two quantities η and η_h are not identical: this corresponds to the fact that convective motions resulting from differential heating in the vertical direction, captured by η, cannot be described by η_h.

4. Estimation of the thermodynamic properties of PCMDI/CMIP3 climate models

The theory developed in the previous sections is applied to analyse the thermodynamic properties of state-of-the-art Climate Models (CMs) using the publicly available output from the PCMDI/CMIP3 dataset (http://www-pcmdi.llnl.gov/). We have used 100 years long time series of monthly means of surface temperature and of radiative fluxes (long-wave and short-wave) at the surface and at the top of the atmosphere, from the PI control run scenario. The PCMDI/CMIP3 dataset includes data from over 20 CMs, but only 14 CMs were considered in this analysis, due to lacking of some fields and/or inconsistencies in the dataset. Models making use of flux adjustments have been excluded too, since they provide an unphysical representation of the thermodynamics of the climate system. See table 3 for the list of models which have been used in this paper. Each model is labelled with a number as in Lucarini and Ragone (2010).

In PI conditions, all the parameters of the model are kept constant (in particular the CO2 concentration is fixed at 280 ppm), so that the slowest forcing acting on the system is given by the

seasonal cycle (the solar cycle, albeit very weak, is considered in some models). Therefore, integrating the model over a sufficiently long time period, the system should reach a stationary state. Once the steady state is reached, the minimal time averaging windown over which one can expect time-independent statistical properties is given by one year. In the following, the time-averaging operator $\overline{(\bullet)}$ used throughout the formulas derived in this paper is considered to act over one year. The consideration of one hundred years for each CM allows constructing a suitable, robust statistics for the yearly-averaged thermodynamical properties of the corresponding climate.

In general, the stationary state of a non-equilibrium system is characterized by vanishing global balances of energy and entropy (Lucarini 2009) and by time-independent statistical properties for the state variables of the system. While this second condition is fulfilled by the climate models here considered, basically by definition of PI control run, the first condition is, in general, not satisfied, as investigated in Lucarini and Ragone (2010), where significant biases have been found in the global energy balances of the system and of its principal subsystems for these models in PI conditions. Nevertheless, as discussed below, it is still possible to take care of such unphysical biases in a similar way as done in Lucarini and Ragone (2010) when computing the meridional enthalpy transport.

There are algebraically different ways to define the yearly value of the emission temperature field T_E. The easiest way is to take:

$$T_E = \sqrt[4]{\overline{LW}/\sigma} \tag{23}$$

where $\overline{LW}$ is the spatial field of annual mean of the longwave emission at TOA. Another possibility is to take for each year T_E as the average of the emission temperature fields T_E^m defined through the

longwave emission as in the previous equation but considering several subsets of the year, e.g. the twelve months. In this case:

$$T_E = \overline{T_E^n} = \overline{\sqrt[4]{LW^n/\sigma}} \quad (24)$$

A third alternative is to take T_E as the inverse of the annual mean of the inverse of the T_E^n, since the multiplicative factor to the annual mean of the radiative balance in Eqs. (8) and (9) is $1/T$, so that:

$$T_E = \left(\overline{1/T_E^n}\right)^{-1} \quad (25)$$

Thanks to the presence of a fourth square root and to the fact that fluctuations of the temperatures are relatively small, the results discussed below are basically unchanged considering any of these definitions, so that the emission temperature T_E results to be a robust descriptor of the system. We have chosen the last option as our standard.

Rather than considering the actual surface temperature fields provided by the CMs, in order to be consistent with the idea of estimating the thermodynamics properties starting from radiative fields only, the considered surface temperature field T_S has been computed from the outgoing longwave radiation at surface by mirroring the procedure described above for computing the 2D T_E fields starting from the TOA outgoing longwave radiation, thus assuming an unit value for emissivity everywhere and at all times. We have verified that the consideration of the surface temperature fields given as outputs by the CMs impacts our results in an entirely negligible way.

The presence of a spurious bias in the TOA global energy balance has been automatically cured

subtracting at each grid-point in each year the globally averaged TOA global energy imbalance. This is a standard procedure when inferring the meridional enthalpy transports, as discussed in Carissimo et al. (1985) and Lucarini and Ragone (2010), and it is justified by the fact that the global energy imbalance at each year is small if compared to the latitudinal variability of the energy balance (of the order of 1 Wm^{-2} vs. 100 Wm^{-2}), which is the quantity we are mostly interested into. When considering entropy estimators, it is especially important to remove the bias in the TOA energy balance, because the related relative error on the estimate of the horizontal component of the material entropy production would be large.

In the case of the net radiative balance at the surface we do not have a zero-sum constraint (latent and sensible heat are not involved in our calculations) because, on the contrary, the typical value of the net global radiative balance at the surface is of the order of 100 Wm^{-2}. Thus, it is not possible to define a bias by observing the violation of the zero mean constraint. In any case, even if the bias were of the order of 10 Wm^{-2}, the resulting error in estimating the vertical contribution to the material entropy production would be (see below) of the order of 5%, so that we can safely ignore it.

We have then computed for each model the yearly value of the total material entropy production $\overline{\dot{S}_{mat}}$, of its vertical and horizontal components $\overline{\dot{S}_{mat}^{ver}}$ and $\overline{\dot{S}_{mat}^{hor}}$, of the equivalent temperatures $T_E^<$ and $T_E^>$, of the baroclinic efficiency η_h, and of the lower bound to the intensity of the Lorenz energy cycle $\overline{W_{\min}}$. From the obtained 100-year time series we have then estimated the expectation value and the confidence interval of the mean of each quantity using the block-bootstrap resampling technique (see, e.g., Lucarini and Ragone (2010)). For all the considered time series the standard deviation is very small, so that the width of the 95% confidence interval is in all cases below 1% of the expectation value. In Table 1 we provide estimates of the expectation values of the

considered thermodynamic parameters.

4.1 Mean values

For explanatory purposes, in Fig. 2a-b we present maps of the average rate of material entropy production by vertical and horizontal processes, respectively, while in Fig. 2c we show the field of emission temperature T_E. All outputs are obtained from CM 13, even if all CMs give similar pictures. In the rest of the paper CMs are labeled with numbers as in Table 3.

In Fig 2a we observe that, consistently with the discussion in Section 2.3, the spatial field whose integral gives $\overline{\dot{S}_{mat}^{ver}}$ is positive everywhere except in small areas at high elevation and latitude where very small negative contributions are obtained. These unphysical results are due to the large temperature inversion observed in these areas, which somewhat compromises the scaling analysis we have adopted. In any case, the global effect of these contributions is entirely negligible. As expected, high values are observed where intense evaporation is present, as in the warm pool of the western Pacific and Indian Ocean, whereas, consistently, very low values are observed in the cold tongue of the Eastern Pacific, near western boundary currents, and in the temperate and cold oceans, while the Mediterranean Sea stands out as a warm pool. Land areas typically feature much lower values than ocean areas at similar latitudes, except for areas characterized by warm and moist climate, such as in the equatorial forests of Amazon, Congo, South-Eastern Asia, where water is always available for evaporation and ocean-like values are obtained. The relevance of the vertical latent heat transport in determining the entropy production is also clarified by the fact that values close to zero are found in deserts (Sahara, Kalahari, Central Asia, Southwestern US and Mexico, Southern Australia, Patagonia), even if intense sensible heat exchanges take place, and in mid-high latitudes terrestrial areas. At polar latitudes, vanishing values are obtained since convective processes are very weak and moisture is

almost absent.

Figure 2b shows that the global value of material entropy production due to horizontal processes results from the (almost perfect, see below) compensation between positive and negative values, with the former dominating the mid-high latitudes and the latter present in the equatorial and tropical regions. Interestingly, some of the features observed in Fig. 2a are found also here: the areas of vigorous moist convection appear as areas of strong negative values related to divergence of (mostly) latent heat. It is also important to note that deserts feature positive values, as they cannot contribute to the latent heat transport and are characterized by high albedo.

Figure 2c shows that, generally, lower (higher) emission temperature T_E are found in the $A_<$ ($A_>$) area, which clarifies that $T_E^{>} > T_E^{<}$ (see below). Nonetheless, local violations to the simple rule "$A_>$→hot & $A_<$→cold" are found. In fact, the Intertropical Convergence Zone (included in $A_>$) features relatively low emission temperatures, since deep convection creates LW radiation-opaque clouds at very high altitude, whereas, conversely, over deserts (included in $A_<$) very high emission temperatures are found, because of the low cloud coverage.

In Fig. 3 we present a scatter plot of the globally averaged, annual mean values of its vertical and horizontal component superimposed on the isolines of the total material entropy production. The error bars represent the 95% confidence interval of the estimate. Models are labeled with numbers as in Table 3. We can see that, apart from model 10, the typical value of the annual material entropy production is between 52 and 58 $mWm^{-2}K^{-1}$. These figures match well with the approximate estimate by Ambaum (2010).

Nevertheless, since our method of computing entropy production relies on several assumptions and approximations, it would be important to check the accuracy of our approach against the values

obtained with the direct method described above. This is possible for CM 13, whose entropy budget has been extensively analysed in Pascale et al (2010) in the same conditions as in the PI scenario here considered. Our estimate of 54.0 $mWm^{-2}K^{-1}$ for the material entropy production is in excellent agreement with the correct value of 51.8 $mWm^{-2}K^{-1}$. This single test is highly encouraging in suggesting that our approximate approach provides an accurate guidance and rather stringent estimates of the actual material entropy production of the system.

The contributions to material entropy production due to vertical and horizontal processes typically amount to about 50 $mWm^{-2}K^{-1}$ and about 5 $mWm^{-2}K^{-1}$, respectively, so that the contribution due to vertical processes is dominant by about one order of magnitude. Figure 3 suggests that the anomalously high total material entropy production of CM 10 is due to a large contribution due to vertical processes, while the contribution to horizontal component is consistent with the values of the other models. In Lucarini and Ragone (2010), CM 10 was found to be the only model with a negative annual global oceanic energy balance. This suggests that an excess of energy is transported into the atmosphere, mostly due to convective processes, with a resulting positive anomaly in entropy production.

CM 6 features a small horizontal component of the material entropy production compared to the other models, even if this does not impact substantially the value of the total material entropy production, given the small weight of the contribution of the horizontal processes. In Lucarini and Ragone (2010), CM 6 was found to have the position of the peak of the annual meridional enthalpy transport located anomalously near the equator with respect to the other models (most notably in the northern hemisphere). This is consistent with CM 6 having a small material entropy production from horizontal processes, since in this model most of the transport is realized at lower latitudes, where the

meridional temperature gradient is smaller.

In Fig. 4 we present a scatter plot of $T_E^<$ and $T_E^>$ together with the corresponding isolines of the efficiency η_h, which are almost indistinguishable from straight lines. We can see that models feature values of $T_E^<$ between around 240 and 244 K, and values of $T_E^>$ between around 255 K and 260 K, so that the typical equivalent temperature difference is about 15 K. Lucarini and Ragone (2010) proposed that spurious positive energy imbalances at steady state due to inconsistencies in the treatment of energy exchanges throughout the climate system induce the presence of a cold bias when emission temperatures are considered. In agreement with this, in the present analysis we find that colder CMs are for the most part those featuring rather large positive global energy imbalances in Lucarini and Ragone (2010), whereas the warmer CMs feature average global energy balances close to zero.

Most models feature values of the efficiency η_h between 0.050 and 0.060, with few models in the range 0.040-0.050 on one side and 0.060-0.065 on the other side. Since CMs differ much more on $T_E^>$ than on $T_E^<$, the largest and smallest efficiencies are related basically to very high and very low values of $T_E^>$, respectively, so that the low latitudes seem to have a prominent role in determining the efficiency of the baroclinic engine. By comparing the figures reported in Table 1 on the value of $\overline{F} = \left\langle \overline{R} \right\rangle_> \left| A_> \right|$ and the sum of the peaks of the meridional transports in the northern and southern hemispheres given in Lucarini and Ragone (2010), we find that the meridional heat transport provides for all CMs a contribution of about 95% to the total transport from radiatively warmer to radiatively cooled areas of the climate system. Therefore, the interpretation of η_h as the baroclinic efficiency introduced by Barry et al. (2002) is definitely appropriate.

In Table 1 we also provide for all CMs the estimates of the lower bound to the intensity of the Lorenz energy cycle for all considered CMs, computed according to Eq. (15). Most values span the

range 1.0-1.5 Wm^{-2}, which definitely captures the right order of magnitude of the Lorenz energy cycle (Peixoto and Oort 1992). Fortunately, the scientific literature provides some benchmarks to be used to test how stringent our bounds are. In the case of CM 13, Pascale et al. (2009) reports that the intensity of the Lorenz energy cycle is about 3.1 Wm^{-2} in simulations mirroring exactly the PI conditions simulation considered here. This implies that the lower bound underestimates the actual value by 60%. In the case of CM 4, CM 18 and CM 20, Marquez et al. (2010) provide estimates for the intensity of the Lorenz energy cycle of 2.7, 3.1 and 3.3 Wm^{-2}, respectively, even if the data are referred to XX century simulations rather than PI conditions. Nevertheless, since relatively small changes of CO2 concentration seem to impact only marginally the Lorenz energy cycle (Lucarini et al. 2010b, Hernandez-Deckers and von Storch 2010), we conclude that also for these models the lower bound underestimates the actual value by around 60%. These results suggest that our approach is fundamentally correct and the theoretically obtained lower bound provides a good zero-order approximation of the actual value of the intensity of the Lorenz energy cycle.

4.2 Variability

We now analyse the mutual correlations of the time series of the yearly values of some of the thermodynamic parameters we have derived, in order to improve our understanding of the dynamical processes keeping the system at a well-defined stationary state. Our time series are 100 years long and feature very weak memory, so that in all cases the 95% confidence interval on the estimates of the correlations has a half-width of 0.2.

First, we look at potential feedbacks of the system. In Fig. 5 we present a scatter plot of the correlation between the yearly time series of the baroclinic efficiency of the system η_h and of the total large scale horizontal transport $F = \langle R \rangle_> A_>$ versus the correlation of the yearly time series of

the horizontal and vertical contributions to the material entropy production. The uncertainty range of the null-hypothesis is represented by the cross centered in (0,0). We find that nearly all the models feature a statistically significant positive correlation between the horizontal and vertical components of the material entropy production, even if the range of values is quite wide. This implies that there is not such a thing as compensation between the two components, with positive anomalies of one component typically corresponding to negative anomalies of the other component, thus determining a negative feedback minimizing the variability of the total material entropy production. On the contrary, it is apparent that during the years where the total material entropy production has, e.g. a positive anomaly, both components change accordingly. Considering also Fig. 2a-b, one may guess that the variability of moist convection in the tropics, which gives the dominant contribution to the vertical component of the entropy production (Lucarini et al. 2010b), drives the variability of the total material entropy production. The positive covariance of the two components of the material entropy production implies that their ratio has a small variability, which, following the discussion presented in subsection 3.2, suggests that the degree of irreversibility α and the Bejan number *Be* are well-constrained parameters of the system. The only qualitative exception is CM 10, which features a borderline statistically significant negative correlation between the vertical and the horizontal components. Combing this result with the evidence given above on the anomalously high value of material entropy production due to vertical processes (see Fig. 3), we propose that CM10 might feature some peculiarities in the treatment of vertical exchange processes (basically convection) and in their coupling with large scale processes responsible for horizontal transport.

Looking at the x-axis in Fig. 5, we discover that among CMs the values the correlation between $\bar{F}$ and η_h span a rather wide range, with the majority of models featuring a statistically significant negative correlation. Since the efficiency is a normalized measure of the equivalent temperature

difference between the warm and the cold box, it is also an integrated measure of the effective meridional temperature gradient realized at the stationary state. Therefore, the presence of a negative correlation between the efficiency and the meridional total transport suggests that a negative feedback acts to dampen large fluctuations of the meridional temperature gradient, in broad agreement with the baroclinic adjustment theory by Stone (1978b). Nevertheless, we observe that for several models the coupling between the two main major features involved in the large scale re-equilibration process - the heat transport and the temperature gradient – is quite weak. These findings seem to be only partially in agreement with the presence of a feedback keeping $\overline{\dot{S}_{mat}^{hor}}$ near an extremum, as implied by the MEPP hypothesis (Kleidon and Lorenz 2005).

Since the value of $\overline{\dot{S}_{mat}^{hor}}$ is proportional to the product of F times the temperature difference between the warm and the cold box (see Eq. (19)), and since the correlation between F and η_h is in general not very strong, it seems of relevance to check out which of the two factors F and η_h is more strongly correlated to $\overline{\dot{S}_{mat}^{hor}}$. This would help answering the question on whether the variability of the entropy production is driven more by the temperature differences or by the total heat flux.

In Fig. 6 we see that all CMs feature a very strong positive correlation between the horizontal component of the material entropy production and the efficiency. All values are above 0.7 and several CMs feature correlations above 0.9. Instead, the correlation with the total transport spans over a larger set of values (from -0.5 to 0.6), so that qualitatively different properties are found among CMs. Surprisingly, only a minority of CMs feature a statistically significant positive correlation between $\dot{S}_{mat}^{hor}$ and F. Therefore, the presence of an anomalously high efficiency or, equivalently, of a high equator-to-pole temperature gradient is definitely a better statistical predictor of high entropy production due to horizontal processes. This result suggests that simplified parameterisations of entropy production

could be written efficiently in the form $\dot{S}_{mat}^{hor} = \dot{S}_{mat}^{hor}(\eta_h)$, which provides further evidence of the relevance of the efficiency parameter introduced here.

These results definitely suggest that, as opposed to the climatological averages considered above, CMs are much less consistent with each other in the representation of the second moments of the large scale thermodynamical properties. This hints at the need for further explorations of the related climate feedbacks.

5. Observational Estimates: Earth, Mars, Titan, Venus.

The computation, or at least the estimation of $\overline{F}$, $T_E^{>}$, $T_E^{<}$, η_h, $\overline{\dot{S}_{mat}^{hor}}$, and $\overline{W_{\min}}$ requires only a very limited amount of data, of much coarser resolution than what considered in the previous section. It is necessary to know only the (net) integrated incoming shortwave radiation and outgoing longwave radiation at the top of the atmosphere in the two areas of positive and negative net radiative balance ($A_>$ and $A_<$, respectively), and use the Stefan-Boltzmann law to derive the relevant temperatures. Alternatively, it is necessary to know the globally averaged incoming radiation, the globally averaged albedo, and the net average radiative budget at the top of the atmosphere in $A_>$ or in $A_<$. We note that, with respect to the case where we can/want to exploit the full 2D fields, when using integrated data a slight cold (stronger warm) bias is introduced when evaluating $T_E^{>}$ ($T_E^{<}$), because in the correct definition given in Eq. (16), emission temperatures are weighted according to the absolute value of net radiative budget. Therefore, the contributions coming from the equatorial is dominant in determining $T_E^{>}$, and, similarly, $T_E^{<}$ happens to be mainly determined by the temperature of the polar regions. As a consequence, integrated data will provide a slight underestimation of the efficiency η_h,

and, consequently, of $\overline{\dot{S}_{mat}^{hor}}$, and $\overline{W_{\min}}$. Note that, since the latitudinal variations of the emission temperature profile are much gentler in the low latitudes, the resulting bias for $T_E^{>}$ should be rather small.

We wish to present a preliminary, but hopefully instructing, example of how it could be possible to obtain information on the thermodynamical properties of celestial objects for which only a very coarse resolution observations of radiative fields at the top of the atmosphere is available. We have then considered the observative radiative datasets provided by Goody (2007) for Earth, Venus, Mars, and Titan and the knowledge of the geometrical radius of each of these celestial objects. We also take the simplifying but reasonable approximation that for in each celestial bodies $A_>$ and $A_<$ have identical size and have a purely zonal structure. This implies that only meridional large scale transports are considered, with the effect of underestimating the value of $\overline{F}$.

It is valuable to compare the figures obtained for Earth with what obtained in the previous section for the CMs runs. Obviously, the comparison is not exactly appropriate because the simulations refer to PI conditions and the observations are taken in the satellite era, but, as discussed in Lucarini et al. (2010b), the variations of the large scale thermodynamic parameters are not very rapid with the changes in the CO_2 concentrations (even assuming a re-equilibrated state), so that we can draw at least qualitative conclusions.

We first note that the $T_E^{>}$ derived from observations is in the upper range of the values simulated by models, the observed value of $T_E^{<}$ is out of the range of values given by the CMs by about 5 K, resulting in a relatively warm *cold reservoir*. Instead, the value of $\overline{F}$ is in the lower range of the values given by the CMs. Consistently, the observational data give for η_h, $\overline{\dot{S}_{mat}^{hor}}$, and $\overline{W_{\min}}$ values which are in the lower range of the CMs results (and very similar to those given by CM 6). Considering

the combined effect of the bias introduced in the estimate of the emission temperature and transport from coarse resolution data discussed above, and the fact that global warming impacts heavily the albedo of the high-latitude regions by reducing its value between PI and XX century data, we can say that a more than satisfactory agreement is found, and that coarse resolution data on planetary bodies can be of great relevance for studying their thermodynamic properties.

Whereas we have several estimates of the material entropy production and of the intensity of the Lorenz energy cycle of the fluid envelope of the terrestrial system, no estimates of these fundamental thermodynamical quantities for the other planets could be found in the literature. Therefore, our bounds could provide useful guidance. Results are reported in Table 3.

We observe that Mars has the largest baroclinic efficiency η_h, as it has a large meridional temperature gradient for the emission temperature. Therefore, in spite of a relatively weak meridional transport, which is hindered by the fact that this planet has a rather thin atmosphere and by the relatively weak irradiance, the lower bound to the Lorenz energy cycle (as well as that to the material entropy production) per unit area is only about one order of magnitude smaller than the Earth's. Since the atmospheric mass per unit area in Mars is about two orders of magnitude smaller than that of our planet, we deduce that the Martian bound per unit mass is higher than that of the Earth.

Instead, the very thick (average surface pressure is about 90 times the Earth's) atmosphere of Venus manages to flatten out the meridional gradient of the emission temperature thanks to relatively strong large scale heat transports $\overline{F}$, in such a way that a rather small value of η_h is realized. Consequently, the material entropy production due to horizontal processes $\overline{\dot{S}_{mat}^{hor}}$ is relatively low (especially considering the huge mass of the atmosphere) and so is the corresponding lower

bound $\overline{W_{\min}}$ to the intensity of the Lorenz energy cycle. Since Venus features an Hadley cell-like pattern of circulation extending to the poles (basically because rotation is negligible) with weak surface winds, our estimates might be informative even if our 2D analysis captures only a limited portions of the contributions to the thermodynamics of the system.

In the case of Titan, the relatively thick (average surface pressure is about 1.5 times the Earth's) atmosphere manages to reduce greatly, thanks to Hadley-cells of large scale circulation, the radiative imbalance between the warm and cold parts of the satellite, so that a only small temperature gradient is realized. Anyway, the much lower values for the thermodynamic bounds $\overline{\dot{S}_{mat}^{hor}}$ and $\overline{W_{\min}}$ with respect to the three analysed terrestrial planets depend mainly upon the much weaker incoming radiation.

5.a Energy Scaling

The differences in thermodynamical properties of the considered celestial bodies are mainly due to the discrepancies in the value of the globally averaged absorbed solar energy, which can be approximately expressed as $S/4(1-\alpha)$, where S is the average solar irradiance along the trajectory of the planet, and α is the average albedo, with the geometrical factor 4 taking care of the ratio between the surface of the planet and the area of its cross section.

If a hypothetical universal thermodynamics of celestial bodies existed and if the only determining factor were the energy input, the thermodynamics of all celestial bodies would be identical once we have the proper scaling properties expressing how the values of the thermodynamic parameters as a function of the energy input. Of course, we do not believe that such universal properties exist, but, in order to compare the thermodynamic properties of the different celestial

bodies *modulo* the energy input, we need to remove, at least at first order, the effect of the differential energy input.

The scaling laws can be derived as follows. The Stephan-Boltzmann law suggests that $T_E^<, T_E^> \sim \left(S(1-\alpha)\right)^{1/4}$, while dimensional analysis hints at $\overline{F} \sim S(1-\alpha)$. Using Eq. (18), we obtain that $\eta_h \sim \left(S(1-\alpha)\right)^0$, while Eq. (17) and Eq. (19) imply that $\overline{W_{\min}} \sim S(1-\alpha)$ and $\overline{\dot{S}_{mat}^{hor}} \sim \left(S(1-\alpha)\right)^{3/4}$, respectively.

We can exploit these scaling properties for a more intrinsic evaluation of the differences in the properties of the circulation of planetary atmospheres. For simplicity, the Earth is taken as reference system, so that in Table 4 we report for each planet *P*, in correspondence to the thermodynamic parameter Φ mentioned above ($\Phi = T_E^<, T_E^>, \overline{F}, \eta_h, \overline{\dot{S}_{mat}^{hor}}$), the nondimensionalized value $\tilde{\Phi}_p$. The nondimensionalized values are defined as $\tilde{\Phi}_p = \Phi_p / \Phi_e \left[S(1-\alpha)\right]_e^\alpha / \left[S(1-\alpha)\right]_p^\alpha$, where Φ_p is the actual physical value of the parameter, and the exponent α changes with the choice of Φ according to the scaling given above (e.g. $\alpha = 1/4$ if one considers $\Phi = T_E^>$) . Therefore, all the rescaled thermodynamic parameters for the Earth have unitary values.

We find that the terrestrial fluid envelope is characterised by the largest values of $\overline{\dot{S}_{mat}^{hor}}$ and of $\overline{W_{\min}}$, but all celestial bodies, in spite of their huge differences in terms of physical and chemical properties, feature values within one order of magnitude. It is also interesting to observe that the three bodies with thick fluid envelope (Earth, Venus, and Titan) have very similar rescaled values of meridional enthalpy transport, which may suggest a “saturation effect”. Mars, due to its thin atmosphere, features a rather weak transport, but, since temperature differences are large, the values of $\overline{\dot{S}_{mat}^{hor}}$ and of $\overline{W_{\min}}$ are comparatively large.

6. Conclusions

In this paper we have performed a re-examination of material entropy production in a general planetary system by proposing theoretical advances and by presenting new results derived from control runs of state-of-the-art GCMs and from the corresponding climate change experiments, as well as from coarse-resolution observative data of Earth, Venus, Mars and Titan.

We have first discussed various approaches recently discussed in the literature for analyzing the entropy budget in the climate system and concluded, from the critical appraisal of recent results presented by Pascale et al. (2009), that the simplified approach of considering a “dry” description of a “moist” atmosphere (Romps 2008), where water is treated mainly as a passive substance which provides/removes latent heat, is well suitable when studying the material entropy production.

We have introduced an approximate splitting between material entropy production contributions due from vertical processes, mostly related to convection and characterized by short time scales, and those due eminently to horizontal processes, mostly g related to the large scale motions in the climate system and characterized by longer time scales. Notably, such an approach allows for computing up to very high precision the material entropy production of the climate system using only 2D radiative fields at the top of the atmosphere and at surface. By comparing our approximate formulas results with the “quasi-exact” treatment by Pascale et al. 2009, we find that our 2D, simplified calculations are correct to within 4%.

We have derived bounds to basic thermodynamical properties of the climate system based only upon time averaged TOA radiative data only. This can in principle be particularly promising especially when one deals with planetary objects, such as distant extra-solar planets, where the

amount of observational data is limited. We have proved that the material entropy produced by the horizontal large scale enthalpy transports, whose divergence is equal to the net radiative budget at the top of the atmosphere, when long term averages are considered (Lucarini and Ragone 2010), is a lower bound to the total material entropy production and, in particular, to its portion related to the dissipation of mechanical energy. From this, a lower bound is derived for the average rate of the Lorenz energy cycle. The Lorenz energy cycle results to be larger than the product of the net input of radiative energy in the positive energy balance regions times a suitably defined baroclinic efficiency, proportional to the difference between the average emission temperatures of areas of the planet with positive and negative radiative balance at the top of the atmosphere. This provides a generalization of the idea that the atmospheric circulation can be described as resulting from a baroclinic heat engine extracting work from the meridional heat flux (Barry et al. 2002). As the meridional heat flux by atmospheric eddies contribute substantially to the total meridional heat flux and, at the same time, play a fundamental role in the Lorenz Energy cycle by transforming zonal into eddy available potential energy, the presence of such constraints is not so surprising.

We have also proved that the product of the lower bound of the intensity of the Lorenz energy cycle times the derived upper bound to the Bejan number gives the product of the actual Lorenz energy cycle times the actual Bejan number.

When the temperature structure of the planet fluid envelope has no vertical structure, it is possible to prove that the inequalities translate into approximate equalities, so that our methods allows for reconstructing basically all large scale thermodynamic properties of the system. This also clarifies the relevance of 2-box models representative of planetary circulations discussed in, e.g., Lorenz et al. (2001). These models, by neglecting vertical processes, cannot provide a plausible description of the material entropy production of a planetary system, nor can be used to test MEPP.

Instead, a minimal model of material entropy production in a planetary system (schematically depicted in Fig. 1) requires at least four boxes, representing cold and warm pools of fluid and cold and warm surfaces beneath, and taking care of representing both horizontal and vertical transport processes.

The evaluation of the contributions to the material entropy production due to horizontal and vertical processes on state-of-the-art GCMs runs provides rather interesting insights. We discover that models agree within about 10% on the value of total material entropy production, and specifically, the disagreements are within about 10% on the value of the vertical term, which is the largely dominant one, whereas larger disagreements (of the order of 20%) exist on the horizontal term, which is about one order of magnitude smaller. Two models seem to be somewhat out of this picture. CM 10 presents a much higher value (by about 20%) of the total material entropy production, where the discrepancy is mostly due to a large overestimate of the contribution due to vertical processes. This hints at some problems in the representation of convective processes, whose parameterisation is especially problematic in a coarse resolution model such as CM 10. Quite reassuringly, the figure we obtain for the total material entropy production for CM 10 agrees with what found by Goody (2000) in a similar version of the same model. Instead, CM 6 presents an anomalously low (by about 30%) value of the material entropy production due to horizontal processes. This may depend on the fact that this model features a peak of the meridional heat transport located anomalously close to the equator with respect to the other CMs considered here (Lucarini and Ragone 2010), so that heat transport takes place among fluid masses of more uniform temperature.

As the entropy production due to horizontal processes can be interpreted as resulting from the large scale heat transport from low (warm) to high latitude (cold) regions, its intensity depends at first order on the product between the maximum intensity of the meridional transport times the

differences between the emission temperature of the two regions. Obvious physical balances would suggest that the two factors should be, model-wise, negatively correlated, so that one expects that the agreement among CMs should be better for the entropy production rather than for the transport diagnostics. Instead, in Lucarini and Ragone (2010) it is shown that discrepancies on the total (and atmospheric) meridional transports among models are also around 20% - it could be argued a role is played by disagreements on their meridional gradients of albedo (see Probst et al. (2010) for a related analysis on total cloud cover). As a result, the baroclinic efficiency of the models disagrees substantially, as do the lower bounds to the intensity of the Lorenz energy cycle. For the CMs where independent data on the intensity if the Lorenz energy cycle are available, we find that such bounds are relatively stringent (within a factor of about 2), which supports the relevance of our theoretical results.

We have then explored the second moments of the thermodynamic parameters discussed above by looking at the properties of their correlations, in order to grasp some understanding of the large feedbacks acting on the system. We discover that CMs disagree quantitatively to a much greater extent than when looking at climatological values of the thermodynamic parameters. Anyway, a robust feature of most models is the positive correlation of the contributions to material entropy production due to vertical and to horizontal processes. The variability of the moist convection in the tropics seems to be the common driver of both contributions. This suggests that no compensation mechanism is in place to *control* the total material entropy production. Similarly, most models feature a negative correlation between the intensity of the large scale heat transport and the difference between the effective emission temperatures of the radiatively heated and cooled areas of the planet, in broad (but far from exact) agreement with the theory of baroclinic adjustment. Finally, we discover that such temperature difference (or, equivalently, the baroclinic efficiency of the system) is

much stronger proxy for the material entropy production due to horizontal processes than the heat flux, thus suggesting its great relevance of large scale indicator of the climate system.

We have then applied our analysis to four specific celestial objects, namely the Earth, Mars, Venus, and Titan, and provided actual estimates for the baroclinic efficiency, the material entropy production due to horizontal processes, and the lower bound to the Lorenz energy cycle. We have used data with the lowest possible resolution compatibly with the goal of studying out-of-equilibrium properties, as we have considered for each planet only two regions, those where the TOA balance is negative and positive, respectively. This ensures that entropy production and the related bounds are underestimated, as an effect of coarse graining. Note that the results by Aoki (1983), who computed the total entropy production of several celestial objects, is not very informative for the thermodynamical properties of the fluid envelope, as the estimates are largely dominated by the (dynamically irrelevant) thermal degradation of radiation (Wu and Liu 2009). In the case of our planet, the bounds are obeyed both in observation and in model data, whereas in the case of the other celestial objects they could, in absence of accurate direct estimates of these thermodynamical parameters, be of useful guidance. In particular, we expect that our lower bounds could closely approximate the actual value of the thermodynamic quantities in the case of celestial objects with thin atmospheres, as in the case of Mars.

Interestingly, once we suitably rescale the values of the thermodynamic parameters in order to take into account the rather different values of energy input from the Sun, we discover that for all celestial objects the values of the thermodynamical bounds are within an order of magnitude, even if the actual masses of the atmospheres vary by around four orders of magnitude, and the Rossby numbers also widely differ.

Future investigations will move along the following lines. First, it would be of great interest to

study how the increase of greenhouse gases impacts the details of the material entropy production on Earth by taking advantage of the PCMDI/CMIP3 dataset. While we expect an overall positive sensitivity of such thermodynamic parameter - see Lucarini et al. (2010b) – it will be interesting to analyse how climate change effects the contributions to material entropy production due to vertical and horizontal processes. Preliminary analyses on the SRESA1B scenario runs suggest that the impact has opposite sign for the two terms, with an increase in entropy production due to vertical processes increases in all CM. This anticipated result, which is apparently at odds with the positive covariability of the annual time series described above in the PI run, casts further doubts in the straightforward applicability of the properties of the natural variability of the climate system properties for inferring the properties of long term, forced climate variations (Lucarini 2008b,2009b). As suggested by the maps showing the spatial properties of the thermodynamic fields considered in this work, the theory presented in this paper can be used also for devising diagnostic tools to be used to analyze local processes and specific geographical features of the climate.

Second, a detailed examination of the Lorenz energy cycle and entropy production of the other celestial objects discussed here (Mars, Titan, Venus) seems of great relevance for its own sake and for understanding the relevance of the thermodynamical bounds proposed here. It is encouraging to note that various models belonging to the PLASIM family (Fraedrich et al. 2005) have already been adapted to study the atmospheres of Titan (Grieger et al. 2004) and Mars (Stenzel at al. 2007).

Third, it would be important to reconcile the definition of thermodynamic efficiency proposed by Johnson (2000) and Lucarini (2009) with that proposed by Ambaum (2010). In this direction, concepts borrowed from endoreversible thermodynamics (Hoffman et al. 1997) could be of great help.

Finally, a theoretical effort will be directed at understanding how to reconcile in this context

the statistical mechanical formula of physical entropy production of a non-equilibrium system in contact with several heat reservoirs at different temperatures, which is proportional to minus the sum of all the Lyapunov exponents of the system (Gallavotti 2004), with the macroscopic formulas used in this publication. This may prove of interest for developing theoretically more refined approaches for analysing the thermodynamics of the planetary systems.

Bibliography

Ambaum M.H.P., Thermal Physics of the Atmosphere, Wiley, New York 2010

Aoki I. 1983: Entropy productions on the earth and other planets of solar system, J. Phys. Soc. Jpn., 52, 1075-1078

Barry L., Craig G. C., and Thuburn J., 2002: Poleward heat transport by the atmospheric heat engine, Nature 415, 774-777

DeGroot S., Mazur P., Non-equilibrium thermodynamics, Kluwar, Dover, 1984

Dewar R.C. 2005: Maximum entropy production and the fluctuation theorem, J. Phys. A: Math. Gen. 38 L371-L381

Emanuel K. A., 2000: Quasi-equilibrium thinking, pp. 225–255 in General Circulation Model Development: Past, Present, and Future, D. A. Randall, Ed., Academic Press, New York

Fraedrich, K., Jansen, H., Kirk, E., Luksch,U. and Lunkeit, F. 2005:. The planet simulator: towards a user friendly model. Meteorol. Zeitschrift 14, 299–304

Fraedrich K., Lunkeit F. 2008: Diagnosing the entropy budget of a climate model. Tellus A 60, 921–931

Gallavotti G.,2004: Entropy production in nonequilibrium thermodynamics: a review, Chaos 14, 680-690

Goody R. 2000: Sources and sinks of climate entropy. Quart. J. Roy. Meteor. Soc. 126, 1953-1970

Goody R. 2007: Maximum entropy production in Climate Theory. J. Atmos. Sci. 64, 2735- 2739

Grassl H. 1981: The climate at maximum entropy production by meridional atmospheric and oceanic heat fluxes, Q. J. R. Met. Soc. 107, 153-166 (1981)

Green J. 1967: Division of radiative streams into internal transfer and cooling to space. Quart. J. Roy. Met. Soc 93: 371–372.

Grieger B., Segschenider J., Keller H.U., Rodin A.V., Lunkeit F., Kirk E., Fraedrich K., 2004: Simulating Titan's tropospheric circulation with the Portable University Model of the Atmosphere, Advances in Space Research 34, 1650-1654

Grinstein G., Linsker R., 2007: Comments on a derivation and application of the 'maximum entropy production' principle, J. Phys. A: Math. Theor. 40, 9717-9720

Held, I.M., 2005: The Gap between Simulation and Understanding in Climate Modeling. Bull**.** Amer. Meteor. Soc., 86, 1609–1614

Hernández-Deckers, D., von Storch J.-S., 2010: Energetics Responses to Increases in Greenhouse Gas Concentration. J. Climate 23, 3874–3887.

Hoffmann K. H., Burzler J. M., Schubert S., 1997: Endoreversible Thermodynamics, J. Non-Equilib. Thermodyn. 22, 311–355

IPCC, Climate Change 2007: The Physical Science Basis. Contribution of Working Group I to the Fourth AssessmentReport of the Intergovernmental Panel on Climate Change [Solomon, S., D. Qin, M. Manning, Z. Chen, M. Marquis, K.B. Averyt, M. Tignor and H.L. Miller (eds.)]. Cambridge University Press, Cambridge, 2007

Johnson D. R., 2000: Entropy, the Lorenz Energy Cycle and Climate, pp. 659-720 in General Circulation Model Development: Past, Present and Future, D.A. Randall Ed., Academic, New York

Kleidon, A., Lorenz, R.D. (Eds.), Non-equilibrium thermodynamics and the production of entropy: life, Earth, and beyond, Springer, Berlin, 2005

Kleidon A., Fraedrich K., Kirk E., Lunkeit F., 2006: Maximum entropy production and the strength of boundary layer exchange in an atmospheric general circulation model, Geophys. Res. Lett., 33, L06706

Lorenz, E.N, 1955: Available potential energy and teh maintenance of the general circulation, Tellus 7, 157-167

Lorenz E.N., The Nature and Theory of the General Circulation of the Atmosphere, World Meteorological Organization, Geneva, 1967

Lorenz R.D, Lunine J.I., Withers P.G., 2001: Titan, Mars and Earth: Entropy production by latitudinal heat transport, Geophys. Res. Lett. 28, 415-418

Li J., 2009: On the extreme of internal entropy production, J. Phys. A: Math. Theor. 42 035002, doi:10.1088/1751-8113/42/3/035002

Lucarini V. 2008a: Validation of Climate Models, in Encyclopedia of Global Warming and Climate Change, G. Philander Ed., SAGE, Thousand Oaks.

Lucarini V. 2008b: Response Theory for Equilibrium and Non-Equilibrium Statistical Mechanics: Causality and Generalized Kramers-Kronig relations, J. Stat. Phys. 131, 543- 558

Lucarini V., 2009: Thermodynamic Efficiency and Entropy Production in the Climate System, Phys Rev. E 80, 021118

Lucarini, V., Fraedrich, K., and Lunkeit, F., 2010a: Thermodynamic analysis of snowball earth hysteresis experiment: Efficiency, entropy production, and irreversibility. Q. J. R. Met Soc. 136, 2-11

Lucarini, V., Fraedrich, K., and Lunkeit, F., 2010b: Thermodynamics of climate change: Generalized sensitivities, Atmos. Chem. Phys. Discuss. 10, 366-3715

Lucarini, V., and Ragone F., 2010: Energetics of PCMDI/CMIP3 Climate Models: Net Energy Balance and Meridional Enthalpy Transport, Rev. Geophys., doi:10.1029/2009RG000323

Marques C.A.F., Rocha, A., Corte-Real, J., 2010: Global diagnostic energetics of five state-of-the-art climate models, Climate Dynamics, 10.1007/s00382-010-0828-9

Martyushev L.M., Seleznev V.D., 2006: Maximum entropy production principle in physics, chemistry and biology, Phys. Rep. 426, 1–45

Mobbs S.D. 1982: Extremal principles for global climate models. Q. J. R. Meteorol. Soc. 108, 535-550

Ozawa H., Ohmura A., Lorenz R.D., Pujol T., 2003: The second law of thermodynamics and the global climate system: A review of the maximum entropy production principle, Rev. Geophys. 41, 1018

Paltridge, G.W., 1975: Global dynamics and climate—A system of minimum entropy exchange, Q. J. R. Meteorol. Soc. 101, 475-484

Paoletti S., Rispoli F., Sciubba E., 1989: Calculation of exergetic losses in compact heat exchanger passages, ASME AES 10, 21-29

Pascale S., Gregory J.M., Ambaum M., Tailleux R., 2010: Climate entropy budget of the HadCM3 atmosphere–ocean general circulation model and of FAMOUS, its low-resolution version, Climate Dynamics, doi: 10.1007/s00382-009-0718-1

Pauluis, O: Entropy budget of an atmosphere in radiative–convective equilibrium. Ph.D. thesis, Princeton University, 274 pp (2000)

Pauluis, O., and I. M. Held: Entropy budget of an atmosphere in radiative–convective equilibrium. Part I: Maximum work and frictional dissipation. J. Atmos. Sci*.,* 59**,** 125–139 (2002a)

Pauluis, O., and I. M. Held: Entropy budget of an atmosphere in radiative– convective equilibrium. Part II: Latent heat transport and moist processes. J. Atmos. Sci*.,* 59**,** 140–149 (2002b)

Peixoto, J.P., Oort, A.H., de Almeida, M. and Tome, A.1991. Entropy budget of the atmosphere. J. Geophy. Res. D6, 10981-10988.

Peixoto, J.P., and Oort, A.H., Physics of Climate. Springer, New York, 1992

Prigogine I., Non-Equilibrium Statistical Mechanics, Wiley, New York, 1962

Romps D.M.: The Dry-Entropy Budget of a Moist Atmosphere, J. Atmos. Sci. 65, 3779-3799 (2008)

Saltzmann B., Dynamic Paleoclimatology, Academic Press, New York, 2002

Shimokawa S. and Ozawa H., 2001: On thermodynamics of the oceanic general circulation: entropy increase rate of an open dissipative system and its surroundings, Tellus A 53, 266-277

Stenzel O.J., Grieger B., Keller H.U., Fraedrich K., Kirk E., Lunkeit F., 2007: Coupling Planet Simulator Mars, a general circulation model of the Martian atmosphere, to the ice sheet model SICOPOLIS, Plan. Space Sci. 55, 2087-2096

Stone P.H., 1978a: Constraints on dynamical transports of energy on a spherical planet. Dyn. Atmos. Oc., 2, 123–139.

Stone P.H., 1978b: Baroclinic adjustment, J. Atmos. Sci., 35, 561–571.

Tailleux R., 2009: On the energetics of stratified turbulent mixing, irreversible thermodynamics, Boussinesq models, and the ocean heat engine controversy. J. Fluid Mech. 639, 339-382

Wu, W., and Liu, Y., 2009: Radiation entropy flux and entropy production of the earth system. Rev. Geophys. DOI: 10.1029/2008RG000275

Table 1: Thermodynamic parameters of PCMDI/CMIP3 climate models in Pre-Industrial conditions.

Models - PI scenario	$T_E^<$ (K)	$T_E^<$ (K)	η_h	$\bar{F}/A$ (Wm^{-2})	$\overline{W}_{min}/A$ (Wm^{-2})	Be_{max}	$\overline{\dot{S}_{mat}^{hor}}/A$ $(WK^{-1}m^{-2})$	$\overline{\dot{S}_{mat}^{vert}}/A$ $(WK^{-1}m^{-2})$	$\overline{\dot{S}_{mat}}/A$ $(WK^{-1}m^{-2})$
1 - BCCR BCM2.0	241.9	257.6	0.061	20.6	1.25	10.0	5.2×10^{-3}	47.2×10^{-3}	52.4×10^{-3}
4 - CNRM CM3	241.5	256.2	0.057	19.2	1.10 [3.1]♦	11.7 [4.1]*	4.6×10^{-3}	49.2×10^{-3}	53.8×10^{-3}
6 - CSIRO Mk3.5	243.8	254.5	0.042	21.7	0.92	14.5	3.8×10^{-3}	51.4×10^{-3}	55.2×10^{-3}
7 - FGOALS	240.1	256.3	0.063	21.0	1.33	10.2	5.6×10^{-3}	52.0×10^{-3}	57.6×10^{-3}
8 - GFDL CM2.0	242.9	257.0	0.055	21.6	1.19	11.3	4.9×10^{-3}	50.5×10^{-3}	55.4×10^{-3}
9 - GFDL CM2.1	243.6	258.0	0.056	21.7	1.21	11.2	5.0×10^{-3}	51.4×10^{-3}	56.4×10^{-3}
10 - GISS AOM	243.1	257.2	0.055	24.0	1.31	12.1	5.4×10^{-3}	60.4×10^{-3}	65.8×10^{-3}
13 - HAD CM3	243.5	259.0	0.060	21.6	1.29 [3.1]♣	10.0 [4.2]♠♣ [4.1]*	5.3×10^{-3}	48.7×10^{-3}	54.0×10^{-3}
14 - HAD GEM	243.4	259.8	0.063	22.6	1.43	9.4	5.9×10^{-3}	50.5×10^{-3}	56.4×10^{-3}
15 - INM CM3.0	243.5	255.5	0.047	23.9	1.13	12.7	4.6×10^{-3}	53.9×10^{-3}	58.5×10^{-3}
16 - IPSL CM4	243.5	258.1	0.057	24.9	1.41	9.5	5.8×10^{-3}	49.5×10^{-3}	55.3×10^{-3}
17 - MIROC3.2 hires	243.4	257.3	0.054	20.5	1.11	12.1	4.5×10^{-3}	50.2×10^{-3}	54.7×10^{-3}
18 - MIROC3.2 medres	242.3	255.9	0.053	21.4	1.14 [2.7]♦	11.2 [4.7]♠♦	4.7×10^{-3}	48.4×10^{-3}	53.1×10^{-3}
20 - ECHAM5/MPI OM	242.8	256.8	0.055	24.6	1.34 [3.3]♦ [2.6]♥	10.4 [4.2]♠♦ [5.3]♠♥	5.6×10^{-3}	53.1×10^{-3}	58.7×10^{-3}

♦ Actual value of the intensity of the Lorenz Energy cycle in XX century simulation runs (Marquez et al. 2010).

* True Bejan number obtained from the entropy production diagnostics reported for the PI simulation run (Pascale et al. 2009).

♣ Actual value of the intensity of the Lorenz Energy cycle in the PI simulation run (Pascale et al. 2009).

♠ True Bejan number computed using Eq. (22) in the text using data of $\overline{W_{min}}$, $\overline{W}$, and Be_{max}.

* True Bejan number obtained from the entropy production diagnostics reported for the PI simulation run (Pascale et al. 2009).

♥ Actual value of the intensity of the Lorenz Energy cycle in the PI simulation run, but using lower resolution (Hernandez-Deckers and Von Storch 2010)

Table 2: Correlations between thermodynamic parameters of PCMDI/CMIP3 climate models in Pre-Industrial conditions. Statistically significant values are depicted in bold, where the half-width of the 95% confidence interval is 0.2.

Models - PI scenario	$C\left(\overline{\dot{S}_{mat}^{hor}}, \eta_h\right)$	$C\left(\overline{\dot{S}_{mat}^{hor}}, \bar{F}\right)$	$C(\overline{F_{max}}, \eta_h)$	$C\left(\overline{\dot{S}_{mat}^{hor}}, \overline{\dot{S}_{mat}^{vert}}\right)$
1 - BCCR BCM2.0	0.81	**0.60**	0.02	**0.51**
4 - CNRM CM3	0.86	0.19	**-0.34**	**0.74**
6 - CSIRO Mk3.5	0.99	**-0.46**	**-0.59**	**0.59**
7 - FGOALS	0.82	**0.38**	**-0.22**	**0.52**
8 - GFDL CM2.0	0.90	**-0.27**	**-0.65**	0.06
9 - GFDL CM2.1	0.70	0.18	**-0.58**	**0.24**
10 - GISS AOM	0.84	0.04	**-0.51**	**-0.20**
13 - HAD CM3	0.78	**0.53**	-0.13	**0.40**
14 - HAD GEM	0.93	0.04	**-0.34**	0.08
15 - INM CM3.0	0.96	**0.36**	0.07	**0.55**
16 - IPSL CM4	0.87	0.18	**-0.33**	**0.61**
17 - MIROC3.2 hires	0.90	**0.23**	**-0.23**	**0.24**
18 - MIROC3.2 medres	0.82	**0.52**	-0.06	**0.56**
20 - ECHAM5/MPI OM	0.88	**0.29**	-0.19	**0.69**

Table 3: Thermodynamic parameters of some celestial objects. Parameters are computed starting from data reported in Goody (2007).

Celestial Body	S $\left(Wm^{-2}\right)$	α	$\lvert A\rvert\left(m^2\right)$	$T_E^<(K)$	$T_E^>(K)$	η_h	$\overline{F}/A$ $\left(Wm^{-2}\right)$	$\overline{\dot{S}_{mat}^{hor}}/A$ $\left(WK^{-1}m^{-2}\right)$	$\overline{W_{\min}}/A$ $\left(Wm^{-2}\right)$
Earth	1373	0.31	5.1×10^{14}	248.3	259.8	0.045	21.0	3.7×10^{-3}	9.5×10^{-1}
Mars	589	0.21	1.4×10^{14}	201.9	222.5	0.093	0.55	2.5×10^{-4}	5.1×10^{-2}
Venus	2624	0.76	4.1×10^{14}	227.9	231.0	0.013	15.2	8.7×10^{-4}	2.0×10^{-1}
Titan	15.2	0.26	8.3×10^{13}	82.8	85.0	0.026	0.24	7.2×10^{-5}	6.1×10^{-3}

Table 4: Same as Table 1, but values are rescaled to terrestrial ones by using the scaling $T_E^<, T_E^> \sim (S(1-\alpha))^{1/4}$**,**

$\eta_h \sim (S(1-\alpha))^0$**,** $\overline{\dot{S}_{mat}^{hor}}/A \sim (S(1-\alpha))^{3/4}$**,** $\overline{W_{\min}}/A \sim S(1-\alpha)$**,** $\overline{F_{\max}}/A \sim S(1-\alpha)$**.**

Celestial Body	$\langle T_E \rangle_<$	$\langle T_E \rangle_>$	η_h	$\overline{F}/A$	$\overline{\dot{S}_{mat}^{hor}}/A$	$\overline{W_{\min}}/A$
Earth	1	1	1	1	1	1
Mars	0.971	1.023	2.09	0.055	0.115	0.115
Venus	1.016	0.985	0.301	1.089	0.328	0.328
Titan	1.010	0.991	0.573	0.963	0.552	0.552

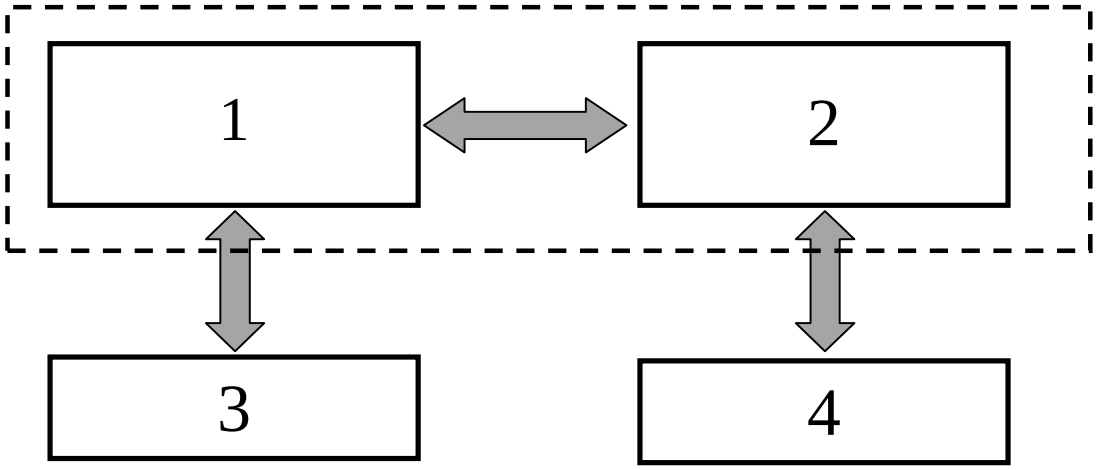

Figure 1: Minimal conceptual for the material entropy production of a planetary systems as deduced from Eq. (9). Boxes 1 and 2 represent warm (low latitudes) and cold (high latitudes) fluid domains, coupled by enthalpy transport. Boxes 3 and 4 represent warm (low latitudes) and cold (high latitudes) surface domains, coupled vertically to the corresponding fluid boxes, but not to each other. The dashed rectangle encloses the reduced two-box model usually considered in previous literature.

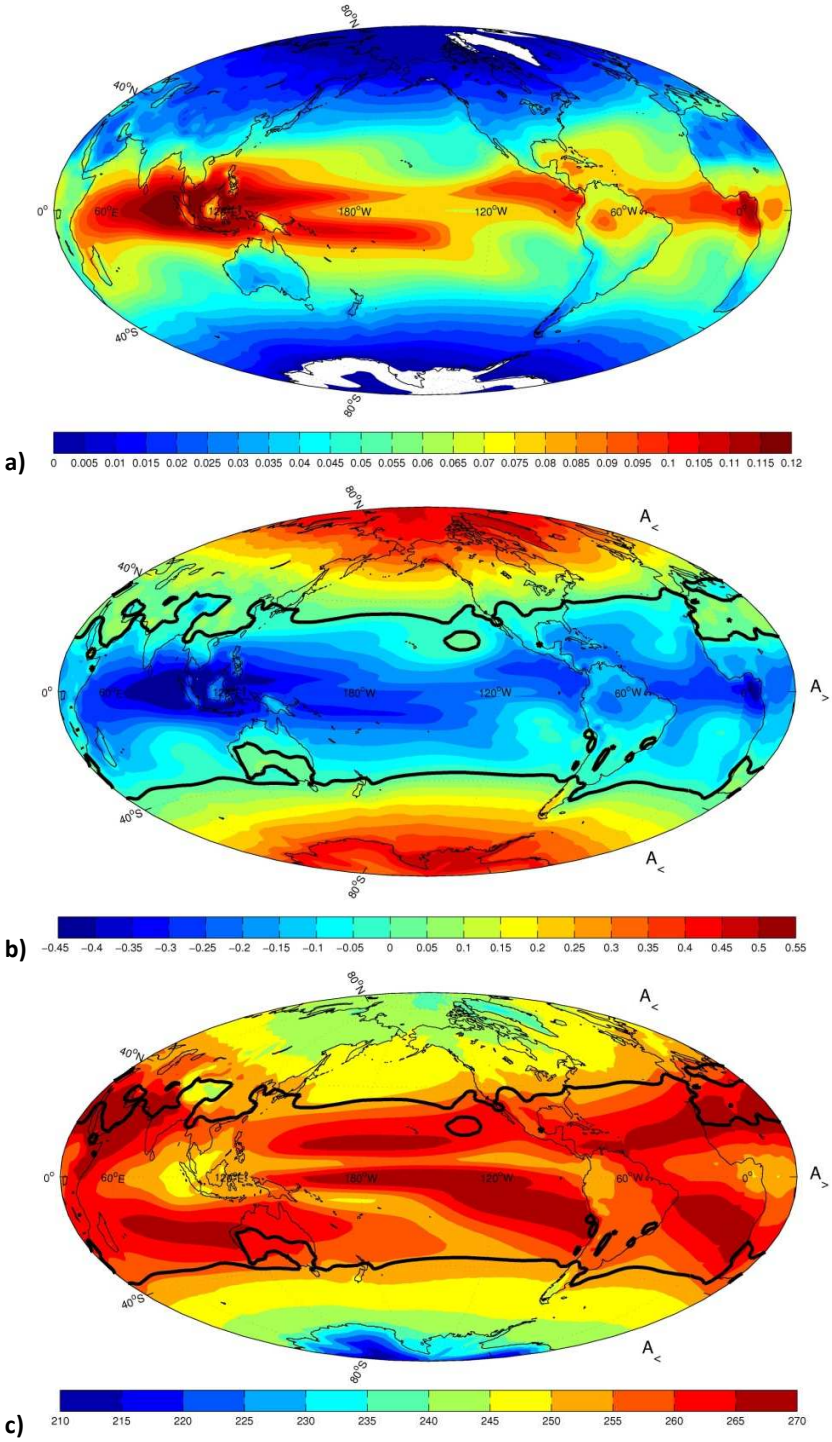

Figure 2: CM 13's average spatial fields of a) material entropy production via vertical processes (values in $WK^{-1}m^{-2}$); b) material entropy production via horizontal processes (values in $WK^{-1}m^{-2}$); c) emission temperature (values in K). In b) and c) the solid black line separates the area $A_>$ with positive net energy budget at TOA from the area $A_<$ where the net budget is negative.

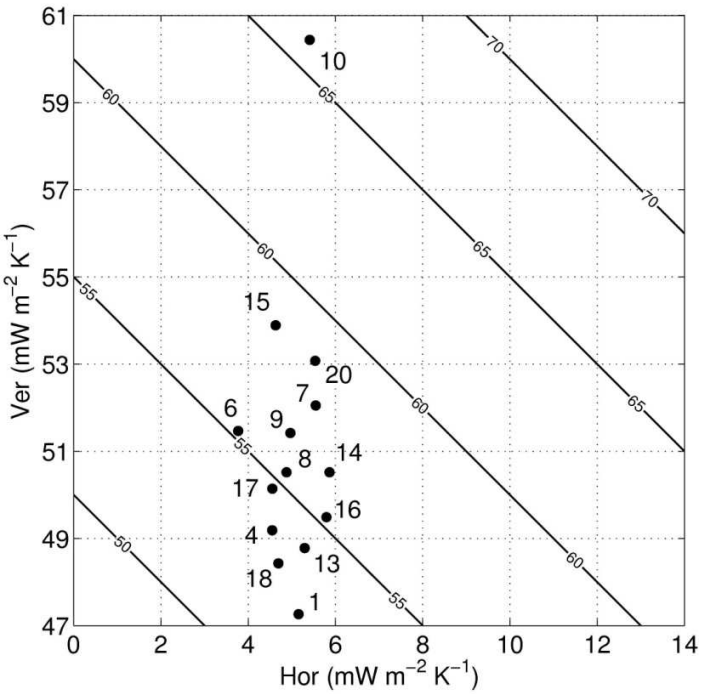

Figure 3: Material Entropy Production in PCMDI/CMIP3 climate models in the pre-industrial scenario runs. The contributions due to horizontal and vertical processes are depicted. Isolines of the total value of the material entropy production are shown as solid lines.

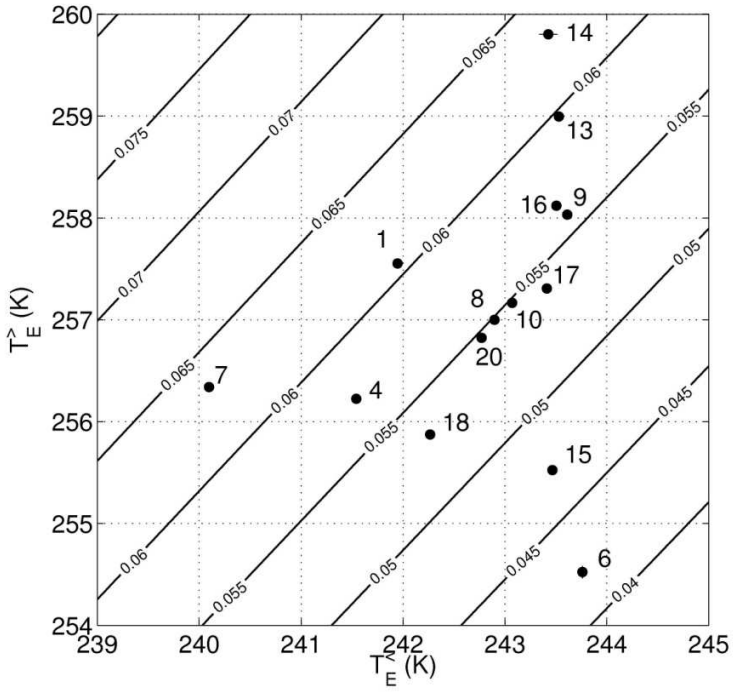

Figure 4: Equivalent temperatures of warm and cold boxes of PCMDI/CMIP3 climate models in Pre-Industrial conditions. Isolines of efficiency are indicated with solid lines.

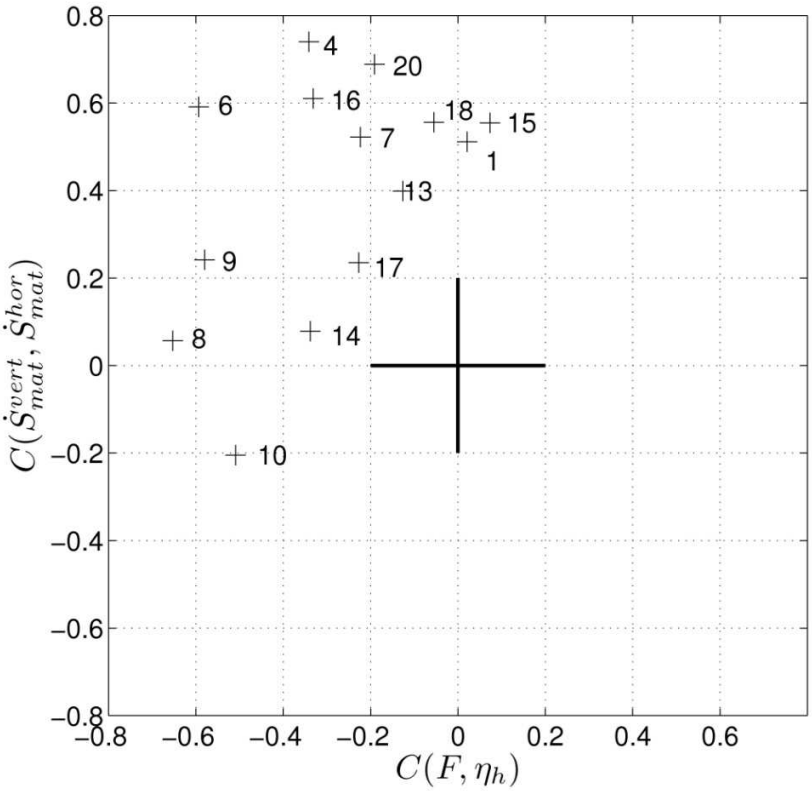

Figure 5: Strength of the large scale thermodynamic feedbacks for PCMDI/CMIP3 climate models in Pre-Industrial conditions. Correlation between total large scale heat transport and the baroclinic efficiency (x-axis) vs correlation between horizontal and vertical components of the material entropy production (y-axis) and and vertical component (y-axis).

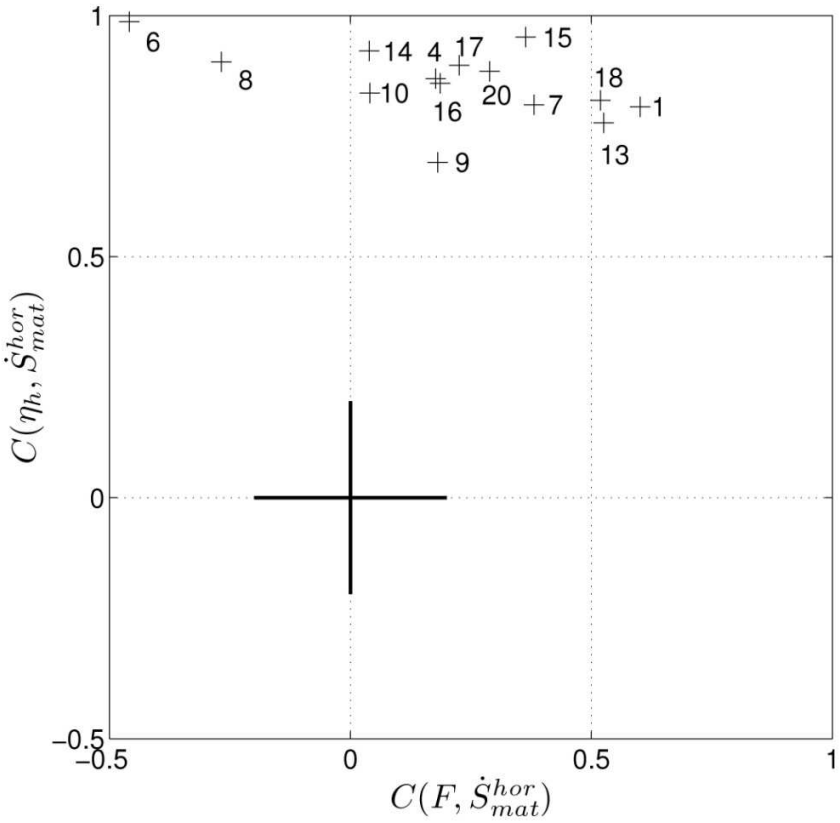

Figure 6: Correlations between horizontal component of material entropy production and total meridional transport (x-axis) and efficiency (y-axis).